Mechanical and genetics basis of cellularization and serosal window closure in Tribolium castaneum

Vazquez Faci, T.

CHAPTER 3

Innexin7 forms junctions stabilizing the basal membrane during cellularization of the *Tribolium castaneum* blastoderm

Tania Vazquez-Faci, Matthew A. Benton, Gerda E.M. Lamers, Chris G.C. Jacobs and Catherine Rabouille, Herman P. Spaink, Maurijn van der Zee*

*An older version of this chapter has been published as:

Van Der Zee, M., Benton, M. A., Vazquez-Faci, T., Lamers, G. E. M., Jacobs, C. G. C., & Rabouille, C. (2015). Innexin7a forms junctions that stabilize the basal membrane during cellularization of the blastoderm in Tribolium castaneum. *Development (Cambridge)*, *142*(12), 2173–2183. https://doi.org/10.1242/dev.097113

Abstract

In insects, the fertilized egg undergoes a series of rapid nuclear divisions before the syncytial blastoderm starts to cellularize. Cellularization has been extensively studied in *Drosophila*, but its thick columnar blastoderm is unusual among insects. We therefore set out to describe cellularization in the beetle *Tribolium castaneum*, the embryos of which exhibit a thin blastoderm of cuboidal cells, like most insects. Using immunohistochemistry, live imaging and transmission electron microscopy, we describe several striking differences to cellularization in *Drosophila*, including the formation of junctions between the forming basal membrane and the yolk plasmalemma. To identify the nature of this novel junction, we used the parental RNAi technique (pRNAi) for a small-scale screen of junction proteins. We find that maternal knock-down of innexin7a (inx7a), an ortholog of the *Drosophila* gap junction gene innexin7, leads to failure of cellularization. RNAseq analysis shows that the pRNAi targeting of innexin 7a had a very strong effect on the transcription of a large group of genes at the egg stage. The results also show feedback on the transcription of various other innexin genes making it impossible to show specificity of the pRNAi approach on innexin 7a. Based on the close homology of the three identified innexin 7 paralogs, we assume that the effects of the pRNAi approach could be the result of silencing of all three paralogs and therefore mention them as the innexin 7 gene cluster. In Inx7 depleted eggs, the invaginated plasma membrane retracts when basal cell closure normally begins. Furthermore, transiently expressed tagged Inx7 localizes to the nascent basal membrane of the forming cells in wild type eggs. We propose that Inx7 proteins forms the newly identified junctions that stabilize the forming basal membrane and enable basal cell closure. We put forward *Tribolium* as a model for studying a more ancestral mode of cellularization in insects.

Introduction

In most insects, the nuclei of the fertilized egg divide multiple times and move to the cortex before cellularization starts. During cellularization, plasma membrane ingresses between the nuclei and encloses them in individual cells (1–3). In *Drosophila*, cellularization comprises different phases: a preliminary phase of membrane ingression, during which the so-called furrow canals are established (see below); a phase of slow membrane extension accompanied by elongation of the nuclei; a rapid phase of membrane extension required for the formation of tall columnar epidermal cells; and final basal closure of the cells by means of actin rings (4). The cells that are formed are tall and narrow.

The formation of the furrow canals during the preliminary phase is a conspicuous start of cellularization in *Drosophila*. The furrow canals are the dilated leading edges of the ingressing membrane to which actin is recruited so that an apical inter-connected hexagonal actin network is formed around each nucleus (5). This network ingresses during membrane extension. The furrow canals are separated from the rest of the ingressing membrane by basal adherens junctions (BAJs). Main components of the BAJs are β-catenin (Armadillo) and E-cadherin (DEcad) (2).

Polarized membrane insertion appears to be the main force driving membrane extension (6). Genes required for cellularization include key regulators of membrane trafficking, such as rab11 and nuf (7–9), and zygotic genes such as *slam* (Acharya et al., 2014) and *nullo*. The latter is involved in the regulation of F-actin at the furrow canals, which is required for stabilization of the cleavage furrow (10). In nullo mutants, some furrows regress during the phase of membrane extension (10).

Whereas cellularization is well studied in *Drosophila*, it is unclear to what extent the molecular mechanisms underlying cellularization are conserved in other insects. *Tribolium* castaneum is a beetle that exhibits traits more ancestral for insects than *Drosophila*, for instance short germ development (11). Also, the thin blastoderm of cuboidal cells seen in *Tribolium* is more typical for insects than the columnar cells of the *Drosophila* blastoderm (12). Hence, we set out to describe cellularization in this beetle using live imaging techniques with transient expression of the membrane marker GAP43-YFP and the filamentous-actin marker LifeAct-GFP (13), immunohistochemistry and Transmission Electron Microscopy

(TEM). We describe several key differences to *Drosophila* cellularization, the main one being the formation of junctions along the forming basal membrane.

To identify the nature of these junctions, we performed a small parental RNAi screen targeting junction proteins, and found that a *Tribolium* ortholog of the *Drosophila* gap junction protein Innexin7 has an essential role in cellularization. Innexin7 function has been studied and appears to have no role in cellularization in *Drosophila* (14–16). Innexins are a family of proteins related to the vertebrate Pannexins (17–20) and functionally similar to the vertebrate Connexins (21–25). Innexins contain four transmembrane (TM) domains, two extracellular loops and an intracellular N- and C-terminus. Groups of 6 protein units assemble into homomeric or heteromeric hemichannels. Interaction in trans of two hemichannels in adjacent membranes is mediated by the conserved cysteine residues in the extracellular protein loops and leads to the formation of a functional gap junction. The first innexins studied were in *Caenorhabditis elegans* (26) and in *D. melanogaster* (27). Later, the Innexins have been found in almost all metazoa (27). Genomic studies have revealed multiple innexin family genes in insect species. In *D. melanogaster*, there are seven genes and in *Tribolium* are 8 innexins (28). The role of innexins has been studied broadly in *D. melanogaster*. For example in the adult visual system, embryonic epithelia organization, morphogenesis, in germ cell differentiation processes, (14) and connection between neurons (29). It is also known that the interactions between the innnexins perform these functions. In comparison, the role of innexins in *Tribolium* has just started to be studied. The only role studied before is from innexin 7 but the role of the other innexins of the best of our knowledge has been not studied.

We performed RNA deep sequencing (RNAseq) to investigate the effect of RNAi knockdown of innexin 7a on the transcriptome. These results show a strong effect on the transcription of genes involved in many fundamental processes such as DNA replication and broad signaling pathways such as the notch pathway. The result could not confirm specificity of the RNAi approach for one particular innexin 7 genes and therefore can only be linked to the entire group of paralogues genes that are highly similar in sequence. Surprisingly RNAi also showed a strong effect on transcription of other innexin genes, including two innexin 7a paralogs. These results indicate a complex feedback mechanism controlled by innexin 7 gene

cluster. At the developmental level we show that RNAi targeting the innexin 7 genes leads to the retraction of the invaginated membrane when basal cell closure normally starts. We propose that Tc-Inx7 proteins forms junctions between the nascent basal membrane and the forming yolk plasmalemma, thus stabilizing the invaginated membrane and enabling basal cell closure.

Materials and Methods

Time-lapse movies

1-2 hours old eggs were dechorionated in 0.5% hypochlorite solution, mounted and injected with 3 µg/µl GAP43-YFP or LifeAct-GFP mRNA as described in Benton et al. 2013 (13). They were then left to develop for 3-4 hours under Voltalef 10S hydrocarbon oil at 32°C, and imaged with a Leica SP5 inverted confocal laser microscope in a heated chamber at 32°C (13). In total we analyzed movies of 22 wild type and 8 Tc-inx7a pRNAi eggs. Six to nine cells per movie were followed and measured in detail for Figure 1M.

Transmission Electron Microscopy

The eggs were incubated in 10% BSA (as a cryo-protectant) and high pressure freezing was performed with a LEICA-EM-PACT2, followed by freeze substitution. Specimens were embedded in Agar 100 resin, sectioned, and examined with a JEOL 1010 Transmission Electron Microscope.

Egg fixation and Immunohistochemistry

Eggs were fixed in a 1:1 4% formaldehyde/heptane mix, devittelinized with a methanol shock, and stored in methanol. Anti-β-catenin/Armadillo (30), anti-Actin (Sigma) or V5 (Invitrogen) antibodies were used 1:1000, 1:50 or 1:1000 respectively in PBS supplemented with 1% BSA overnight at 4°C. After washing, eggs were incubated with anti-rabbit Alexafluor488 at 1:250 in PBS-BSA 1%. For actin staining using

phalloidin, eggs were fixed in 4% paraformaldehyde for 15 minutes and devittelinized using forceps and needle before incubation with phalloidin 1:5000 for 20 min at room temperature. Eggs were mounted in vectashield with DAPI and imaged under a Leica DM6000 epifluorescent, SP5 or SPE confocal microscope.

Parental RNAi for images and videos

dsRNA was synthesized using SP6 and T7 polymerases (Ambion) and injected into pupae according to Bucher et al., 2002 (31). For parental RNAi see Supplementary Table S1 for details. Injection of dsRNA into eggs was performed as previously described for mRNA injection (13).

Phylogenetic analysis

Putative orthologs were identified by BLAST (32). Alignment was made using Praline (http://www.ibi.vu.nl/programs/pralinewww). Parts of the alignment where most sequences had gaps were not taken into account for phylogenetic analysis by creating a mask in Seaview (33). WAG+I+G was the most informative amino acid substitution model according to ProtTest (34). The maximum likelihood phylogeny was generated using PhyML (35) and was edited in MEGA3.1 (36). Accession numbers (NCBI, National Centre for Biotechnology Information) of the used sequences are: XP_002405917=IsInx1; XP_002415523=IsInx2; XP_002405920=IsInx8a; XP_002433826=IsInx8b, XP_002434835=Inx8c; EFX65318.1=DpInx1; EFX65316.1=DpInx2a; EFX77054.1=DpInx2b; EFX74755.1=DpInx3a; EFX74754.1=DpInx3b; EFX65317.1=DpInx7; EFX84089.1=DpInx8; XP_001946431=ApInx1; XP_001944681=ApInx2a; XP_003241809=ApInx2b; XP_001947982=ApInx2c; XP_001949382=ApInx3; XP_003247903.1=ApInx7; XP_001944798=ApInx8; XM_001121323=AmInx1; XM_003251623= AmInx2; XM_623560=AmInx3; XM_624661=AmInx7; XM_396916=AmInx8; XP_001603984=NvInx1; XP_001604034=NvInx2; XM_003427685=NvInx3; XM_001603958=NvInx7; XP_001599753=NvInx8; AGAP001476-PA=AgInx1; AGAP001488-PA=AgInx2; AGAP004510-PA=AgInx3; AGAP006241-PA=AgInx456; AGAP001477-PA=AgInx7; AGAP001487-PB=AgInx8.

Tc-Inx7a-V5 transient expression

The full coding sequence of Inx7a was cloned using the primers 5'-AGA ATT CAC ATG TTG AAA ACT TTC GAA GCG-3' and 5'AAC TCG AGG TCA AAT TTC GCC GGC TTT TTC-3'; digested with EcoRI and XhoI, and ligated into pMT/V5 (Invitrogen) that had been digested by the same enzymes. The fusion construct was excised with PciI and NotI, cloned into the modified expression vector pT7-DsRed (13), linearized with NotI, and in vitro transcribed using the T7 mMESSAGE mMACHINE kit (Ambion). 3µg/µl capped mRNA was injected in 0-2 hours old eggs. Eggs were allowed to develop for 8 hours at 32°C and fixed for staining with the anti-V5 antibody (Invitrogen).

Parental RNAi for RNA deep sequencing

We injected two different parental RNA of interference (RNAi) into adults *of Tribolium castaneum.* The first parental RNAi is the control. It is a *Tribolium* Non-targeting sequence of dsRNA synthesized from the vector pCRII (Invitrogen) using the forward primer 5'-TGCCGGATCAAGAGCTACCAA-3' and the reverse primer 5'-TGTGAGCAAAAGGCCAGCAA-3' (37). The second parental RNA of interference is a sequence to knock down the gene Innexin 7a (TC011061). These dsRNA were made by the company Eupheria . For injection of parental dsRNA. first, 268 females were selected at the pupa stage. Once the females became adults, they were fixed on a microscope slides with a tape at their abdomen. Later, one elytrum was raised to be injected dorsally with parental RNAi (38). We injected 134 adult females with control parental RNAi and 134 adult females with parental RNAi to silence the Innexin 7 gene. The amount of parental RNAi injected per female was about 2 µl of a 0.5 µg/µl. After two days of the injection, adult males were added.

Sample collection for transcriptional analysis

The beetles were on egg laying for 12 hours in fine flour. After, we isolated the eggs from the adults and flour. To separate the adults we used a grid of 800 µm. To remove the eggs from the flour we used a grid of 350 µm. Approximately 300 eggs were obtained. We extracted the RNA from

the eggs using Trizol extraction (Invitrogen). Later, we purified the RNA extracted and digested the DNA on column with the RNeasy kit (Mini Elute). We collected 3 biological samples for each parental RNAi injection. We sent the RNA purified from the eggs to Genomescan company for sequencing.

RNAseq data analysis and bioinformatics

RNA sequencing from the eggs injected with Innexins 7a RNAi and the eggs injected with the control were performed by the company Genomescan, Leiden and passed their internal quality control for RNA (using an Agilent fragment analyzer) and sequence cluster yield. A total of at least 20 million paired end sequencing reads was obtained for each sample. Mapping of the reads was performed using the program Genetiles (39) using the genome assembly version Tcas 5.2. The mapping statistics shows that for each sample at least 70 % of the reads could be mapped and at least 40% of the reads could be mapped with a paired end read. We coupled the Ensembl gene IDs for mapping the reads to those of orthologs of *D. melanogaster* because the *D. melanogaster* database is better annotated than the database of *T. castenum*. As a caveat, it should be mentioned that with this method we could not find orthologs for approximately 30% of the *Tribolium* genes.

To identify the enrichment pathways of the differential expressed genes in the knock downs of Innexin 7 we used the bioinformatics software Database for Annotation, Visualization and Integrated Discovery (DAVID) (40, 41). We upload RNAseq list into DAVID to find the main pathways where these genes play a role. To select the pathways, we used a household of p-value<0.05. DAVID is developed by the Frederick National Laboratory for Cancer Research, United States of America.

We obtained the most enriched pathways of the differentially expressed using PathVisio software (42). PathVisio is developed by Maastricht University, the Netherlands. We used a p-value<0.05.We used PathVisio to discover genes that are expressed differently when we knock down innexin 7. We compared the two pathways list from DAVID and PathVisio and we analyzed the pathways found in both lists. We obtained the pathways from WikiPathways. We used for identifier mapping database the Dr_Derby_Ensembl_91.bridge database that is available at the Pathvisio website. Some pathways have been converted manually using the

Basic Local Alignment Search Tool (BLAST) at NCBI73 and Ensembl to find or confirm the *D. melanogaster* orthologues of the *Tribolium* genes.

Results

To investigate cellularization in *Tribolium*, we followed development using live imaging of embryos in which the cell cortex was labeled with the YFP-fused, GPI-anchored plasma membrane protein GAP43 (43). This fusion protein was transiently expressed by mRNA injection into eggs from wild type beetles or from a transgenic line expressing nuclear-localized GFP (13, 44).

We found that membrane invaginates between the nuclei after the 10th nuclear division (i.e. about 6 hours after egg laying) (Figure 1 A-D'. The 11th division occurs 30 minutes later (Figure 1 A). In contrast to *Drosophila*, the invaginated membrane does not retract and then invaginate anew at each nuclear division. Instead, already invaginated membrane remains at its original depth, just below the nuclei, and a new cleavage furrow invaginates between the daughter nuclei to form two protocells (Figure 1 E-J). One hour after the 11th division, the 12th and last synchronous division takes place (Figure 1 B).

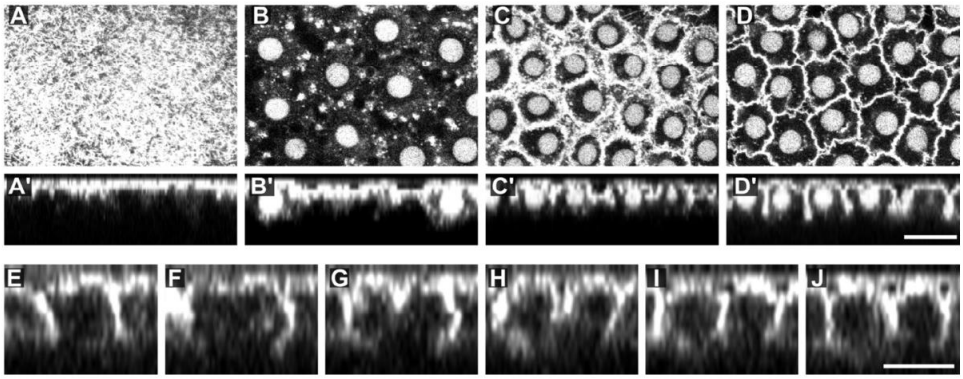

Figure 1. ***Membrane ingression during cellularization. (A-D')*** *Time series of membrane ingression during cellularization in a nuclear-GFP transgenic egg transiently expressing GAP43-YFP as membrane marker, timed from just before the moment that nuclei reach the surface of the egg (shown in A), i.e. after the 10th nuclear division. (A-D) optical sections either at the level of the membrane in (A), or at the level of the nuclei in (B-D). (A'-D') Orthogonal views from same time points. When nuclei are not visible in the orthogonal views it is because the cross section did not bisect them.* ***(E-J)*** *Time series of orthogonal views of membrane ingression during the 12th division in a GAP43-YFP transiently labelled embryo, timed from just before division begins as shown in (D). (E) prior to division a single protocell is visible. (F) when the nucleus divides (not visible) the membrane moves further apart. (G) Following separation of the chromosomes (not visible), membrane begins to invaginate between the new nuclei. (H-I) membrane continues to invaginate between new nuclei. (J) Two new protocells are visible. Scale bars: 20 µM*

About 90 minutes after this last synchronous division (at t≈2h30 after the 11th division), the protocells become refined into a regular array of pentagons and hexagons, with rare tetragons and heptagons (45). This suggests an increase in cortical tension. Concomitantly, a basal membrane starts to form (Figure 2 P, R1-4). Thus, a phase of rapid membrane extension is absent. Thirty minutes later, at t ≈3h, the cuboidal cells have completely closed at the basal side. Finally, at t≈3h30, the closed cuboidal cells of the germ rudiment start to divide asynchronously for the first time, giving rise to the differentiated blastoderm stage (Figure 2). Thus, cell closure in *Tribolium* appears to take place one cell cycle earlier than in *Drosophila*, i.e. after the 12th instead of the 13th division (1–3, 12).

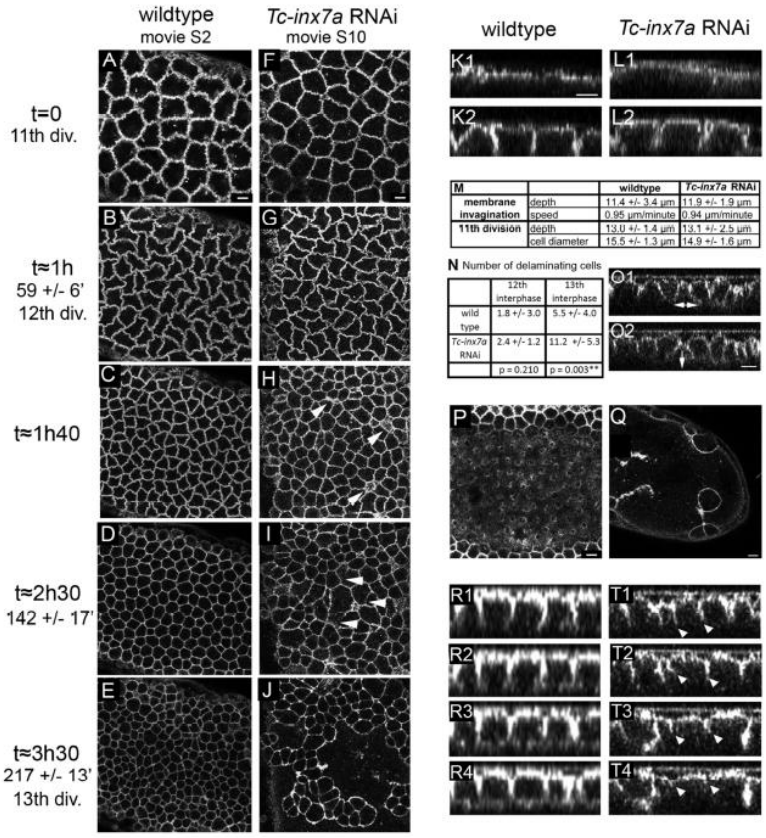

Figure 2. Cellularization in wild type and Inx7a depleted eggs. *(**A-E**) Stills from a time-lapse movie of a developing wild type egg transiently expressing GAP43-YFP as a plasma membrane marker In this movie, t=0 is set at the onset of the 11th division. The 12th division (t=1h) is the last synchronous division and the 13th (t=3h30) is the first asynchronous division of the germ rudiment. **(F-J)** Stills from a GAP43-YFP time-lapse movie of a developing Tc-inx7a pRNAi egg at approximately the same time points as (A-E). Arrowheads in H point at delaminating protocells. Arrowheads in I indicate retracting membrane. **(K,L)** Stills from GAP43-YFP time lapse movies showing the beginning (1) and the end (2) of the plasma membrane ingression after 10th division in wild type (K) and Tc-inx7a pRNAi eggs (L). (**M**) Quantitative measurements of the depth and speed of membrane invagination after the 10th nuclear division, as well as size of the protocells after the 11th division in wild type and Tc-inx7a RNAi eggs (see Materials and Methods). **(N)** Quantification of delaminating protocells in a 145µm x 145µm area before and after the 12th division in 8 wild type and 8 Tc-inx7a pRNAi eggs. **(O)** Lateral views of the process of protocell delamination. During delamination, membrane of a protocell is biased towards neighboring nuclei (O1 double-headed arrow). This protocell is extruded from the epithelium (arrow in O2). (**P**) Still from a GAP43-YFP time lapse movie of a wild type egg (at a basal focal plane at the time of basal closure. **(Q)** Still from a GAP43-YFP time lapse movie of a Tc-inx7a pRNAi egg (). Note the large uncellularized area. **(R, T)** Stills from GAP43-YFP time-lapse movies showing orthogonal views of basal membrane formation in a wild type egg (R) and Tc-inx7a pRNAi egg (T). Arrowheads in T indicate retracting membrane. Note that one cell on the left manages to close in T4. Scale bars: 10 µm. Scale bar in K1 applies to all orthogonal views.*

In Tribolium, furrow canals are not enriched with actin

In *Drosophila*, the leading edges of the ingressing membrane are dilated and form interconnected furrow canals that are enriched with actin and are separated from the rest of the membrane by an Armadillo-rich basal adherens junction (BAJ, see introduction). The described live imaging with the plasma membrane marker GAP43 was not carried out at sufficient resolution to determine whether furrow canals are present in *Tribolium*. To resolve this, we inspected the tips of the ingressing membrane by TEM, and observed dilated bases (Figure 3 A-D, asterisks). Furthermore, as in *Drosophila*, those dilations are separated from the rest of the membrane by junctions (Figure 3 A-D, green arrowheads). To establish if these junctions are BAJs, we used an antibody to localize Armadillo. Indeed, after the 12th division, Armadillo localization is consistent with BAJs above the furrow canal (Figure 3 E). We conclude that furrow canals are also present in *Tribolium*.

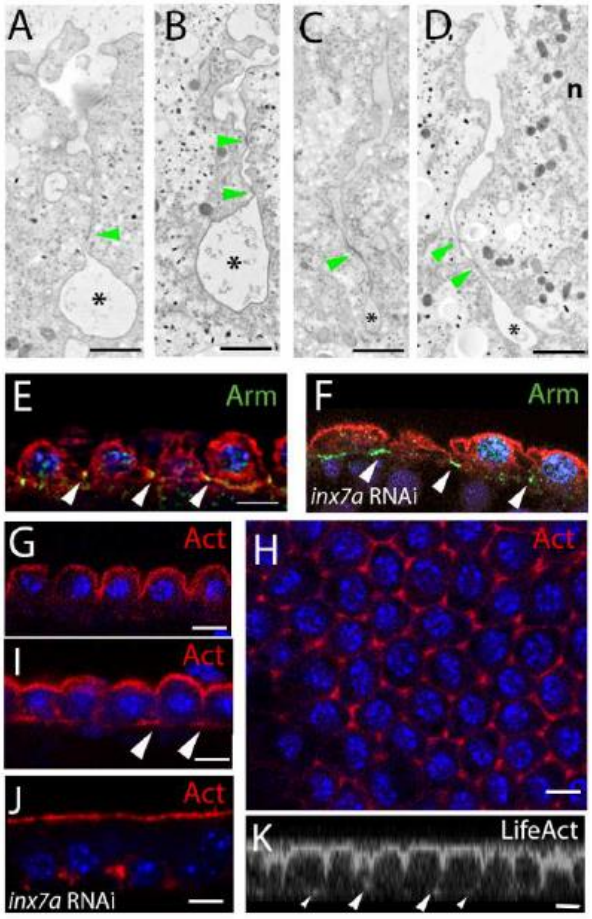

Figure 3. Analysis of the furrow canals in Tribolium. ***(A-D)*** *Transmission Electron Micrographs of ingressing membrane in wild type eggs. Furrow canals are indicated with asterisks. Junctions are indicated with green arrowheads. "n" denotes nucleus in (D).* ***(E, F)*** *Immunofluorescence (IF) visualisation of Armadillo (green) and tubulin (red) and nuclein with DAPI (blue) in wild type (E) and Tc-inx7a pRNAi (F) blastoderm. Note that in F, Armadillo is still detected on some retracting membranes (arrowheads).* ***(G-J)*** *IF visualisation of actin (red), nuclei with DAPI (blue), in wild type (G, I, H) and Tc-inx7a pRNAi (J) blastoderm. No enrichment of actin is observed at the base of the ingressing membrane (G), except for the corners where three cells meet (H, arrowheads in I). A few dots of actin remain basally after Tc-inx7a RNAi (J).* ***(K)*** *Orthogonal view of a LifeAct time-lapse movie revealing minor accumulations of Actin at the bases of some of the ingressed furrows (arrowheads). Scale bars:1µm (A-D); 10 µm (all other panels).*

However, in contrast to *Drosophila*, the furrow canals are not heavily enriched with actin. Neither phalloidin, nor an actin antibody could detect conspicuous actin enrichment at the bases of the ingressing membrane (Figure 3 G). We did detect some basal enrichments of actin when basal cell closure starts (Figure 3 I), but these enrichments correspond only to corners where three cells meet (Figure 3 H). As more membrane is present at these points, this apparent actin accumulation likely reflects normal levels of cortical actin. In order to exclude penetration problems of the actin antibody, we also injected mRNA coding for LifeAct-GFP that specifically labels F-actin (13, 46). Similar to the actin antibody, this revealed minor actin accumulation at the base of some of the ingressed

furrows (Figure 3 K), but incomparable to the well described and consistent localization of actin to all furrow canals in *Drosophila* (5).

Taken together, these results suggest that furrow canals are formed during *Tribolium* cellularization, but they are less enriched with actin than those in *Drosophila*.

Novel junctions form along the nascent basal membrane

After the 12th division, the dilated edges of the ingressed membrane start to enlarge (Figure 4 A-D). Subsequently, the ingressed membrane splits at the basal side as the furrow canals flatten (Figure 4 E, F). Surprisingly, we found that new junctions form between the nascent basal membrane and forming yolk plasmalemma (Figure 4 E, F, red arrow heads). As the basal membrane extends laterally, additional junctions are continuously added, until junctions are present along the whole basal membrane (Figure 4 G, see also supplementary Fig. S1). Such junctions have not been described in *Drosophila*.

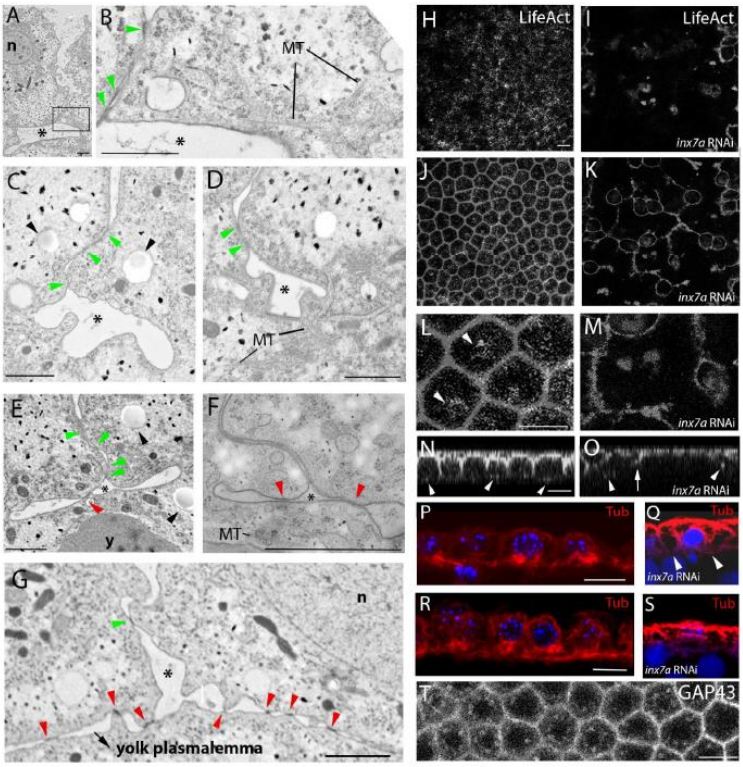

Figure 4. Basal cell closure in Tribolium. (A-D) *Transmission Electron Micrographs showing the enlarging and splitting furrow canals (asterisks). (B) is a magnification of the area boxed in (A).**(E-G)** TEM visualization of both the lateral BAJ (green arrowheads) as well as novel junctions between the nascent basal cell membrane and the forming yolk plasmalemma (red arrowheads, see also Supplementary Fig. S1.) Asterisks indicate the split furrow. n denotes nucleus in (A) and (G). MT denotes microtubuli in (B, D and F). y indicates yolk in (E). **(H, I)** Still from LifeAct-GFP time lapse movies in wild type (H) and after Tc-inx7a RNAi (I) at a basal focal plane. Note the extensive basal network of actin in (H) and its absence in (I). **(J, K)** Overlay of a more apical plane on the stills shown in (H) and (I). **(L, M)** Magnification of (J) and (K). Arrowheads in (L) point at accumulations of actin where the cells constrict. **(N, O)** Orthogonal views of (J) and (K), respectively. Arrowheads in (N) point at presence of actin where the cells constrict. Arrow in (O) indicates retracting membrane; arrowheads indicate remaining dots of actin. **(P-S)** IF visualization of Tubulin around nuclei in wild type (P, R) and Tc-inx7a pRNAi blastoderms (Q, S) presented as overlay of several confocal planes. DAPI (blue) stains the nuclei. Note that in wild type eggs, microtubules appear enriched and condensed during basal cell closure, whereas they retract in Tc-inx7a pRNAi (S).**(T)** Still from GAP43-YFP live imaging showing numerous moving compartments at the basal side of the forming cell.Scale bars: 1µm (A-G); 10 µm (all other panels).*

In *Drosophila*, cell closure is mediated by actin ring constriction (1). Although we could detect these rings using immunofluorescence in *Drosophila* (Supplementary Figure 1 F), we could not detect such rings in *Tribolium*. To exclude penetration difficulties of the antibody, we also analyzed basal cell closure by live imaging of embryos transiently expressing LifeAct-GFP (Figure 4 H, J, L, N). During basal membrane formation, a fine network of actin becomes visible at the base of the forming cells (Figure 4 H). An overlay of a more apical view revealed enrichments of actin at the constrictions of the basal membrane in some protocells (Figure 4 J, L, see Figure 4N for lateral view). However, these enrichments are incomparable to the obvious actin rings in *Drosophila* (Supplementary Figure S1F) and closely reflect the pattern observed with the membrane marker GAP43-YFP (Figure 4 P). This suggests that these actin enrichments represent normal levels of cortical actin, and that the role of the actin cytoskeleton in basal cell closure may not be as prominent as in *Drosophila*.

We did, however, detect enrichment of microtubules at the basal side of the closing cells (Figure 4 P, R). Microtubules are also evident in TEM micrographs (Figure 4 B, D, F). Thus, it is possible that polarized membrane insertion along microtubules plays a role in basal cell closure, like during the phase of rapid membrane extension in *Drosophila*. Consistent with this, we observed numerous highly mobile, GAP43-YFP positive compartments, suggesting extensive membrane activity (Figure 4 T). Furthermore, at the basal sides of the forming cells, TEM revealed conspicuous vesicles with a thin membrane and remnants of homogenous filling (Figure 4 C, E). These are probably lipid droplets and could supply lipids for membrane synthesis. However, we did not functionally test a possible role for membrane insertion in basal cell closure.

Taken together, basal cell closure in *Tribolium* relies on different mechanisms than *Drosophila*. First, the actin pattern found in *Tribolium* is incomparable to the conspicuous actin rings detected in *Drosophila* during basal constriction. Second, junctions form between the nascent basal membrane and the forming yolk plasmalemma. As we do not detect Armadillo at the basal membrane (Supplementary Figure S1E), these junctions are likely not adherents junctions.

TC011061 is an innexin7 ortholog and its maternal knockdown leads to a strong defect in cellularization

In an attempt to identify the nature of the basal junction during cellularization in *Tribolium*, we performed a small parental RNAi screen targeting candidate junction proteins (31). Knockdown of most genes encoding these proteins generated either sterile mothers (such as the E-cadherin knockdown) or mild non-penetrant egg phenotypes (47). In contrast, injection of dsRNA targeting TC011061, a gene with clear similarities to innexins, leads to a consistent and 100% penetrant phenotype in the early development of all eggs. In these eggs, late blastoderm stage nuclei are irregularly spaced when compared to wild type eggs (Figure 5 A-D). Phalloidin staining marking the cell cortex indicates the absence of membrane between many nuclei (Figure 5 E-H), giving the impression of multinucleated cells. Furthermore, some nuclei detach from the apical surface (Figure 5 F). These phenotypes are characteristic of cellularization mutants in *Drosophila* (3).

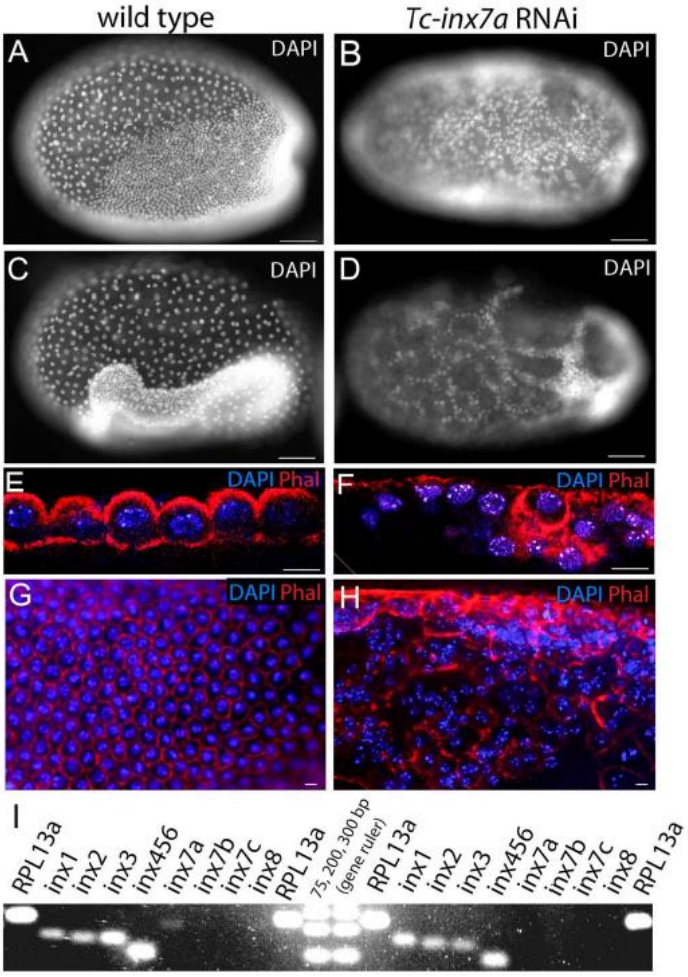

***Figure 5*. *Knockdown of Tc-inx7a leads to a strong cellularization phenotype*(*A-D*)** *Visualisation of nuclei with DAPI of wild type (B, D) and Tc-inx7a pRNAi (C, E) differentiated blastoderms (B, C) and at early gastrulation (D, E). Note in C and E that the nuclei are irregularly spaced. (**E-H**) Visualisation of nuclei (DAPI, blue) and actin marking the cell cortex (phalloidin, red) in wild type (F, H) and Tc-inx7a pRNAi eggs (G, I) by confocal (F, G) and epi (H, I) fluorescence microscopy. Note that cortical actin is absent between most nuclei in G. Note the apparent multinucleated cells in I. In I, the epifluorescent image has been deconvoluted. (**I**) RT PCR on cDNA from 0-6 hours old eggs from wild type and Tc-inx7a dsRNA injected mothers. Tc-inx7a is weakly expressed in wild type eggs, and this expression is absent in Tc-inx7a pRNAi eggs. Ribosomal Protein 13a (RPL13a) was used as reference gene (Lord et at, 2010). See Supplementary Table S2. Scale bars: 50µm (A-D); 10 µm (E-H).*

In total we found eight innexin genes in the *Tribolium* genome, all encoding proteins with the conserved four TM topology, a characteristic YYQW motif in the second TM domain, and the two conserved C residues (Supplementary Fig. S2) (14, 16). To establish the correct orthology of TC011061 and the other innexins, we first generated a Maximum Likelihood phylogeny including arthropod Innexins from available full genome sequences (Figure 6). Although the bootstrap values at the base of tree are low, the crustacean and insect innexins strongly cluster together in clear orthology groups, allowing unambiguous classification of the *Tribolium* Innexins. As in *Drosophila*, single orthologs of innexin1 (*ogre*), innexin2 (*kropf*) and innexin3 are present in *Tribolium*. Whereas the *Drosophila* genome contains the paralogs innexin4 (*zpg*), innexin5 and innexin6, *Tribolium* possesses a single ortholog that we named *Tc-inx456*. In the 3.0 version of the *Tribolium* genome, two *innexin8*-like genes are predicted (TC011065 and TC011066), but upon closer inspection these belong to a single gene that produces two isoforms with different first exons, similar to the *Drosophila* innexin8 shak-B locus (Phelan and Starich, 2001). Finally, our phylogenetic analysis clearly identified TC011061 as an innexin7 ortholog (bootstrap value=93), that we arbitrarily named *Tc-inx7a*, as the *Tribolium* genome contains two other innexin7 paralogs (named *Tc-inx7b* and *Tc-inx7c*). These three genes are close together in a head-to-tail orientation on the chromosome, and their phylogeny suggests that they are innexin7 duplications specific to the *Tribolium* lineage. Since these three paralogues are highly similar in sequence we are not sure that the pRNAi targeting of *inx7a* will lead to specific knockdown.

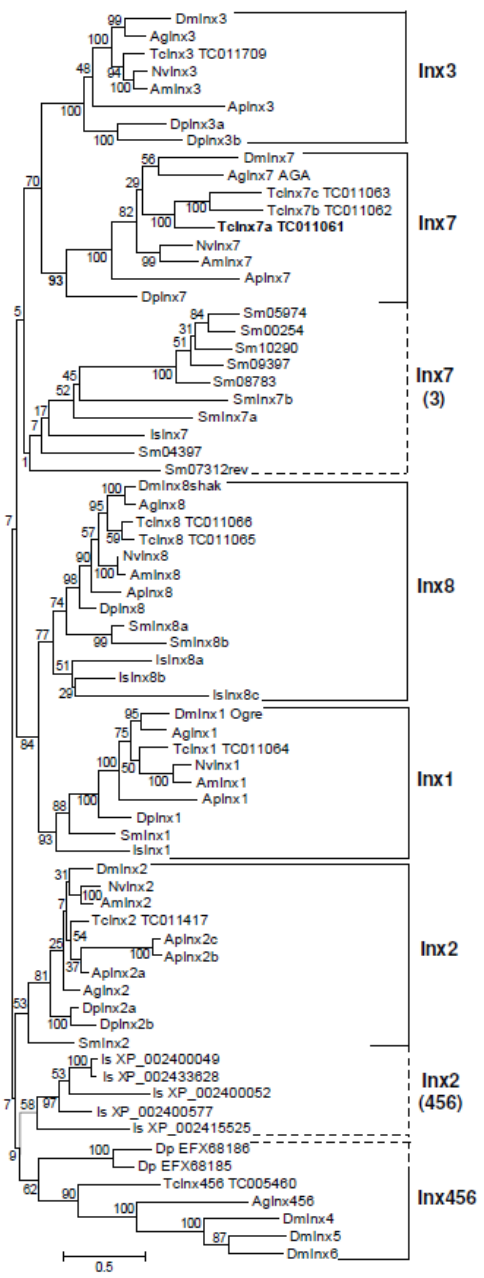

Figure 6. Maximum Likelyhood Phylogeny of the Arthropod Innexins. *Amino-acid substitution model: WAG+I+G, see Materials and Methods. Root was placed arbitrarily. Bootstrap values of 1000 replicates are indicated in percentage. The duplications of the pea aphid inx2 genes confuse the Inx2 branch somewhat. Abbreviations: Sm = the centipede Strigamia maritima; Is = the mite Ixodes scapularis; Dp = the water flea Daphnia pulex; Ap = the pea aphid Acyrthosiphon pisum; Am = the bee Apis mellifera; Nv = the wasp Nasonia vitripennis; Tc = the beetle Tribolium castaneum; Ag = the mosquito Anopheles gambiae; Dm = the fly Drosophila melanogaster. Strigamia maritima numbers are predictions from the preliminary genome sequence. SmInx7a and SmInx7b are named based on synteny in a gene cluster that is incorrectly predicted as one fused gene Sm07312 but consists of SmInx2, SmInx7a, SmInx7b, Inx1 and Inx8a. This synteny is also found in other Arthropods, like Nasonia and seems to be ancestral. Inx3-like sequences would then have arisen in the Pancrustacea. Sm08783, Sm09397, Sm10290, Sm00254, Sm05974 and possibly Sm04397 might be duplications of Inx7, but low bootstrap values do not allow unambiguous identification. Sm07312rev is an Inx7-like gene that has an inverted orientation in the Sm07312 cluster. Sm10724 is a duplication of Inx8a and is named SmInx8b. The mite sequences XP_002415525, XP_002400577, XP_002400052, IsXP002433628 and 002400049 cluster together with Inx456, but could as well belong to the Inx2-group. The latter would be more likely given the presence of Inx2 in the ancestral cluster. The Daphnia sequences EFX_18186 and EFX_68185 cluster together with Inx456. Since this could be due to long branch attraction, these sequences have not been named. Inx456 could thus have arisen in the higher holometabolous insects.*

RNAseq analysis of eggs after pRNAi targeting of innexin 7a

We performed RNAseq of RNA isolated from eggs of which the parents were injected with dsRNA targeting inx7a. The results from the differential expression of genes after pRNAi as compared to the control show a large set of genes that are differentially expressed (Figure 7). Using a P-value threshold of 0.05, a gene set of 1811 genes was identified that was different expressed after knockdown. We coupled the Ensembl gene IDs of these *Tribolium* genes to those of orthologs of *D. melanogaster* because the *D. melanogaster* database is better annotated than the database of *Tribolium* resulting in a list of 2414 *Drosophila* orthologs that were present in DAVID data base.

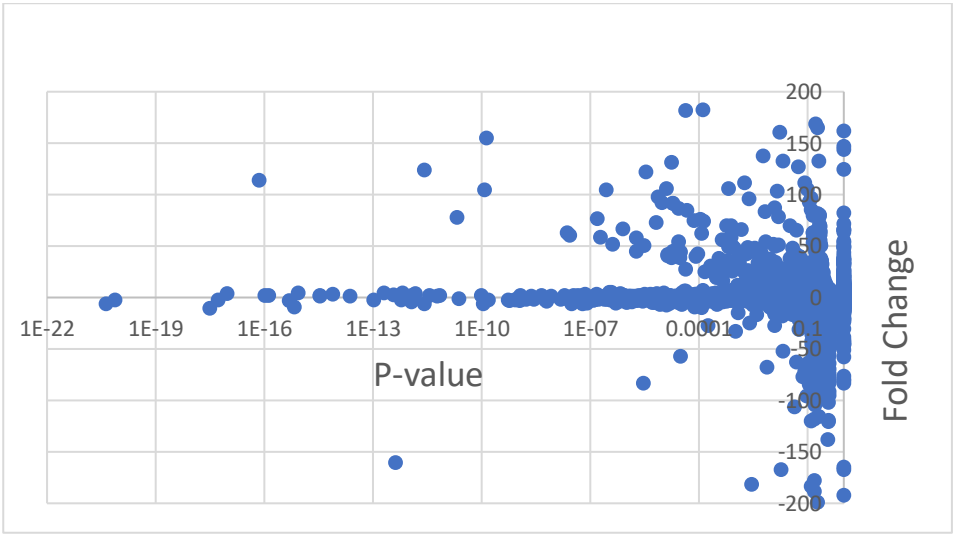

Figure 7. *Volcano plot showing the genes that are up or down regulated.*

We performed gene enrichment analysis of the *Drosophila* ortholog gene set to describe the effects of the pRNAi on the transcriptome. Functional annotation charts obtained from DAVID showed a strong enrichment with very low P values of many genes that are linked to development, particularly linked to insect cuticle development (see Gene Ontology in Table 2). We used two software programs for pathway enrichment analysis: DAVID and PathVisio. For PathVisio analysis we had to annotate manually many genes because they are poorly annotated in the

pathways available from Wikipathways (https://www.wikipathways.org/index.php/WikiPathways). We obtained two very different lists of enriched pathways from each software program (Table 2). The difference can be explained because the software programs uses different databases and algorithms to find the most enriched pathways (40–42). Therefore, as the two lists are different, we present them as complementary data. We focused on two pathways that were present in both lists: Notch signaling and DNA replication pathways.

Table 2. Comparison between the tables from PathVisio and David (KEEG and BP)

DAVID			
KEGG			
pathway	**Counts**	**%**	**p- value (PERMUTED)**
DNA Replication	40	25.7	0.072
Notch Signaling Pathway	16	28.6	0.127
Glycolysis and Gluconeogenesis	41	0.3	0.2
TGF Beta Signaling Pathway	15	0.3	0.125
mRNA processing	87	0.2	0.36
Non-homologous End joining	5	0.3	0.189
GO term			
Biological process	**Counts**	**%**	**p- value (PERMUTED)**
Chitin-based cuticle insect development	86	3.3	1.32E-20
Heterophilic cell-cell adhesion via plasma membrane cell adhesion molecules	25	1.0	9.66E-13
Transmembrane transport	110	4.2	5.90E-12
Flavonoid biosynthetic process	26	1.0	3.63E-11
Flavonoid glucuronidation	26	1.0	3.63E-11
Insecticide catabolic process	20	0.8	2.66E-10
PATHVISIO			
Pathway	**Counts**	**%**	**P-Value**
Endocytosis	105	1.3	4.10E-04
RNA degradation	51	0.6	1.10E-03
Fanconi anemia pathway	26	0.3	6.30E-03
Valine, leucine and isoleucine degradation	30	0.4	9.80E-03
N-Glycan biosynthesis	34	0.4	1.30E-02
DNA replication	33	0.4	1.60E-02
FoxO signaling pathway	47	0.6	1.60E-02
Notch signaling pathway	22	0.3	1.70E-02
Terpenoid backbone biosynthesis	20	0.3	2.70E-02
Pyrimidine metabolism	68	0.9	3.10E-02
beta-Alanine metabolism	18	0.2	4.30E-02
RNA polymerase	27	0.3	5.10E-02
Spliceosome	103	1.3	6.30E-02
Protein export	21	0.3	6.70E-02
Hippo signaling pathway - fly	50	0.6	7.00E-02
Ubiquitin mediated proteolysis	81	1	9.30E-02

We show visualization in PathVisio for the DNA replication pathway (Figure 8). In eukaryotes, DNA synthesis is complex, involving around 60 different proteins, depending on the organism, and therefore only part of it is shown: assembly of the pre-replicative complex (48).

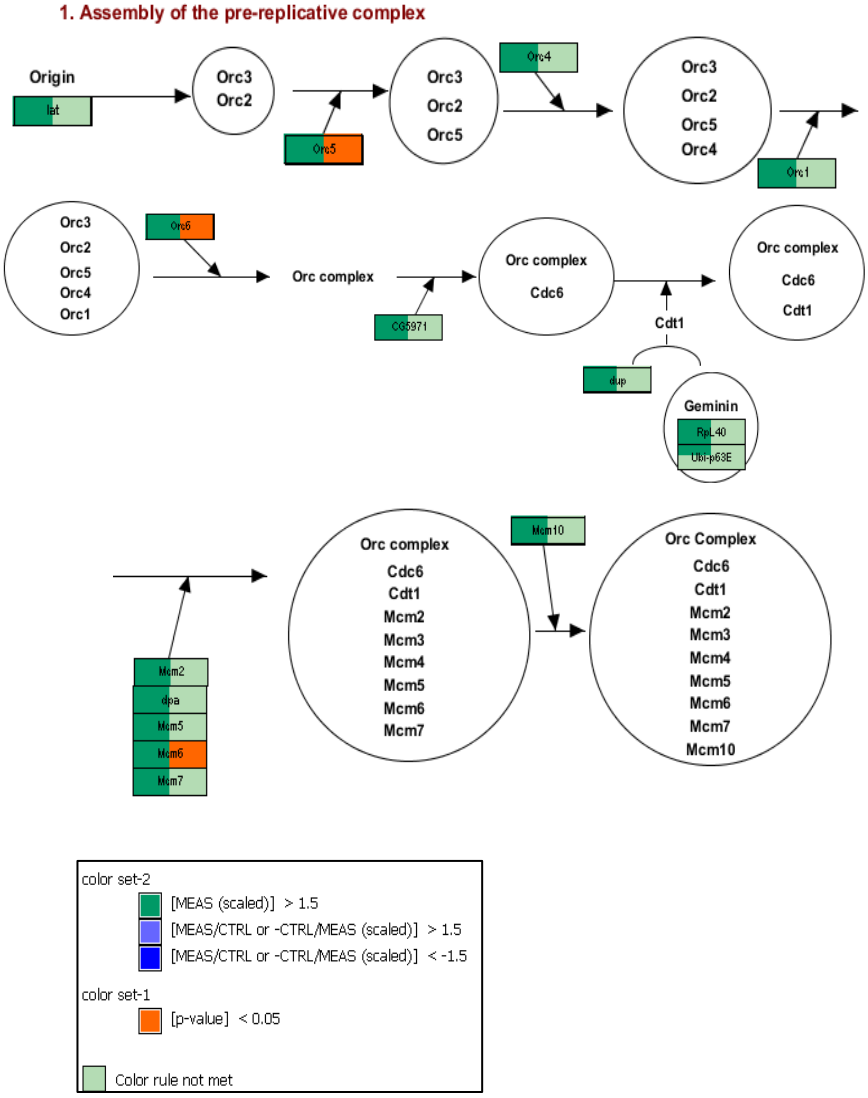

Figure 8. First step of DNA replication pathway using PathVisio for visualization. We did not show the rest of the pathways since there is no difference between the targeted RNAi and the control experiments. In eukaryotes, DNA synthesis is complex because the replication machinery has to deal with many difficulties, for example, specialized DNA structures, chromatin and even damaged DNA. This process involves around 60 different proteins, depending on the organism. DNA replication is related to the cell cycle and only happens once in each cell cycle (48).

We also used PathVisio to visualize the Notch signaling pathway (Figure 9). Notch signals are important in many process of the cell. For example, during development and maintenance of tissues, the Notch signal promote or suppress cell proliferation, cell death, acquisition of specific cell fates or activation of differentiation programs (49).

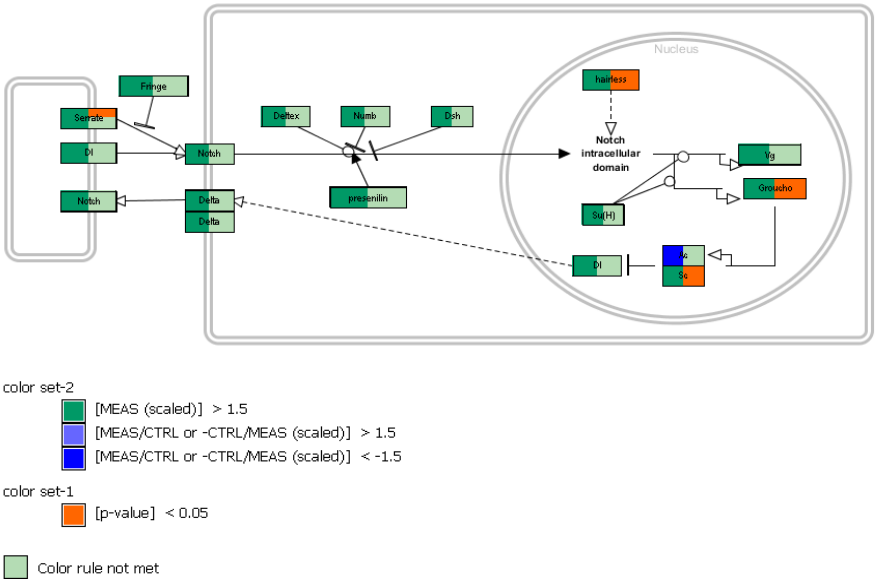

Figure 9. *Notch signaling pathway using PathVisio for visualization. In general, the Notch signaling pathway depends on the ability of a ligand to trigger receptor proteolysis, resulting in delivery of an active Notch fragment. The proteolysis is required for the receptor activation. After the Notch intracellular domain (NICD) is released by proteolysis, it travels to the nucleus. There, the NICD attaches to a DNA binding protein to gather a transcription complex that activates downstream target genes (49).*

In summary, the effect of knocking down inx7a has a strong effect on many pathways. This effect is expected since the knock down resulted in disturbance of cellularization which is a major transformation during embryonic development.

Changes in transcription of all innexin genes after pRNAi targeting of innexin 7a

Unexpectedly, the results show that inx7a is upregulated after pRNAi that targets this gene (Figure 10). This means that there is no evidence for the penetrance of the silencing on the RNA level of the targeted gene itself (Table 3). To analyze if there is a connection between targeting inx7a and the transcription of the rest of the innexins, we compared the level of expression of all the innexins after inx7a targeting (called treatment in the figures) with the control. In Figure 10, we plotted the level expression of the innexins comparing the control (orange) and the treatment (blue). We observed that innexin 7c and 8 (form 1) have very low coverage (in the order of 10 reads) and innexins 1, 2 and 3 have high coverage (in the order of 10000 reads). We performed a t-Test to analyze if there are significant differences in expression between the treatment and control. We observed that innexins 1, 2, 3, 456 and 8 have significantly different expression after treatment. The Innexins 1, 2, 456 and 8 have higher levels of expression than the control. On the contrary, inx3 has a lower level of expression in the treatment than in the control. In conclusion, the innexins 1, 2, 3, 456 and 8 are affected by targeting inx7a and therefore we assume that they have a connection with the silencing of inx7a. Based on the close homology of the three identified innexin 7 paralogs we assume that the effects of the pRNAi approach could be the result of silencing of all three paralogs and therefore we use the generic name innexin 7 (inx7) to indicate the entire gene cluster.

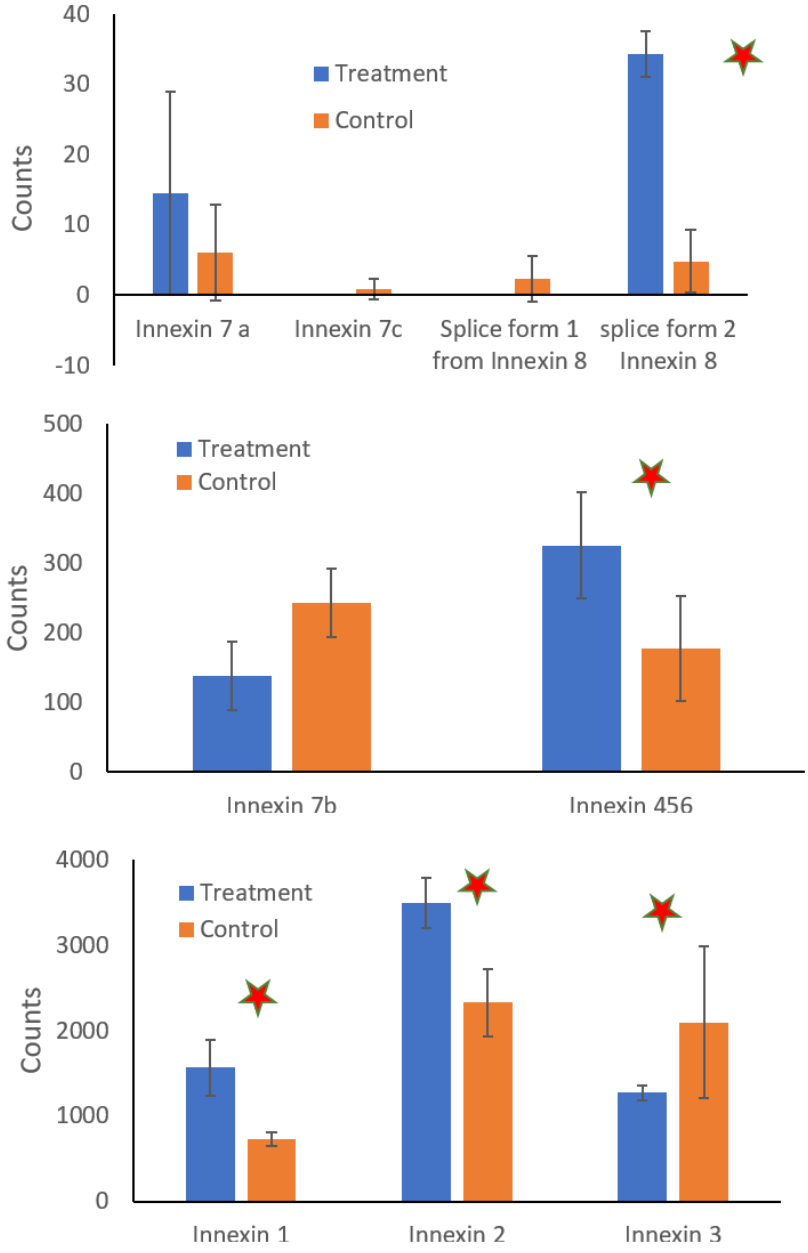

Figure 10. *Level of expression of innexins genes. The star means that the treatment and control are significantly different using a t- test with P-value<0.05. In blue is the treatment (Innexin 7 knocked down) and in orange is the control. Innexin 7c and 8 (splice form 1) have no detectable expression in the three repetitions of the experiment after treatment and also the controls have very low expression making it not possible to measure the effect of the knock down of inx7a.*

Table 3. Regulation of the genes after innexin 7 was silenced.

Name	TC Number	Fold Change	Regulation
Innexin 7 a	TC011061	2.337392808	upregulated
Innexin 7 b	TC011062	-1.648009698	down regulated
Innexin 7c	TC031404	-0.714082731	down regulated
Innexin 1	TC011064	2.197547938	upregulated
Splice form 1 Innexin 8	TC011065	-2.786227456	down regulated
Splice from 2 Innexin 8	TC011066	6.549326031	upregulated
Innexin 456	TC005460	1.936111705	upregulated
Innexin 3	TC011709	-1.502989278	down regulated
Innexin 2	TC011417	1.590002054	down regulated

Inx7 is required to maintain the invaginated membrane after the 12th division

To investigate how maternal knock-down of *innexin7a* leads to failure of cellularization, we compared cellularization of Tc-inx7a knockdown eggs to the wild type using GAP43-YFP live imaging movies. In Tc-inx7a pRNAi eggs, both the depth and speed of membrane invagination at the 10th division are unaltered (Figure 2 K-M,). Similarly, at the 11th division, no differences in depth of the cleavage furrows or diameter of the protocells are observed between wild type and Tc-inx7a pRNAi eggs (Figure 2 F, L, M).

The dramatic phenotype upon Tc-inx7a pRNAi starts to develop after the 12th division. First, directly after this last synchronous division, some protocells delaminate from the epithelium (arrowheads in Fig. 2H;). This also happens to a small extent before the 12th division, but not significantly more often than in wild type (Figure 4 N). After the 12th division, however, Inx7a depleted eggs show a highly significant increase in the number of delaminating protocells, suggesting a general instability of the blastoderm. During delamination, membrane of a protocell becomes skewed towards neighboring nuclei, ending in extrusion of that protocell (Figure 4). Second, ingressed membrane between the protocells strikingly disappears by the time basal cell closure starts in wild type eggs (Figure 4 T). Orthogonal views reveal that this disappearance is in fact a retraction of invaginated membrane to the apical surface (Figure 4 T). This leads to a

complete reversal of the cellularization process and gives rise to large cell-free areas (Figure 4 J). In the strongest cases, close to 100% of the invaginated membrane retracts (Figure 4 Q), and only a few cells have closed basally (Figure 4 Q, T,). In conclusion, in the absence of Inx7, plasma membrane invaginates normally, but retracts when basal cell closure starts.

No evidence for a direct role of Inx7 in BAJ, tubulin or actin localization

As Innexin2 in *Drosophila* colocalizes and interacts with Armadillo (50), we hypothesized that BAJ formation might be affected upon loss of Inx7a, causing destabilization of the ingressed membrane. However, Armadillo localizes normally in Tc-inx7a RNAi knock down eggs and even persists on retracting membrane (Figure 4F). This suggests that Inx7 is not required for BAJ formation and maintenance. Microtubules also appear in the basal part of the cell in Inx7a depleted eggs (Figure 4Q), suggesting that Inx7 does not affect initial formation of the basal microtubules. However, these microtubules never become as prominent as in wild type, and later retract with the retracting membrane (Figure 4S). Given the normal initial formation of microtubules, it is possible that this tubulin retraction is a consequence of the retraction of the membrane rather than its cause. Thus, we could not find evidence that incorrect localization of BAJs or microtubules causes the retraction of the ingresses plasma membrane.

In *Drosophila* cellularization mutants like Discontinuous Actin Hexagons (DAH) or *nullo*, membrane retraction is precipitated by reduced levels of F-actin at the furrow canals (10, 51). As interactions between the actin cytoskeleton and gap junction proteins have been shown for Connexin43 (Crespin et al., 2010; Wall et al., 2007) and the Pannexins (Bhalla-Gehi et al., 2010), we hypothesized that actin might be incorrectly localized upon Tc-inx7a RNAi. Indeed, a basal network of actin does not appear to form in Inx7a depleted eggs (Figure 4 I, K, M, O). In Inx7 depleted eggs, actin is visible at the cortex of the few cells that manage to close (Figure 4 K, M, O), at retracted membrane (Figure 4 O) and in a few basal dots (Figure 4J; Figure 4 K, M, O). However, no differences in actin localization are observed between Inx7a depleted eggs and wild type eggs until basal cell closure should start. This leaves the possibility that the

absence of the basal actin network is a mere consequence of the missing basal membrane, rather than its cause.

Overall, Inx7 is required for the stabilization of the ingressed membrane once basal membrane formation begins. We could find no evidence, however, that Inx7 exerts its function by directly localizing BAJs, microtubules, or actin.

Inx7a-V5 localizes to the basal membrane

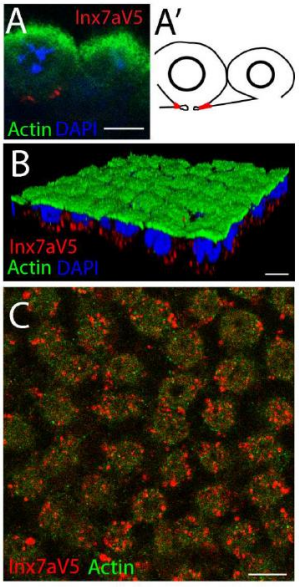

Figure 11. Localization of the transiently expressed Inx7a-V5 fusion protein (A-C) IF localization of transiently expressed Inx7a-V5 (using an anti-V5 antibody; red), actin (anti-actin antibody; green) and nuclei (DAPI, blue). (A) Orthogonal confocal section, showing that Inx7a-V5 localizes to the base of the invagination, where the membrane of the nascent cell and the yolk plasmalemma meet. (A') Schematic drawing of A. (B) 3D opaque reconstruction showing the basal localization of Inx7a-V5. Fixation was optimized for V5 antibody staining, resulting in poor actin antibody penetration that was insufficient to visualize the basal membrane in an opaque 3D reconstruction (C) Confocal section through the base of the forming cells where Inx7-V5 is detected in plaques, mostly overlapping with the basal cortical actin. Scale bars: 10 µm.

Next, we hypothesized that Inx7 is a component of the junctions identified by TEM between the forming basal membrane and the yolk plasmalemma. These junctions could flatten and split the enlarged furrow canal, thus stabilizing the ingressed membrane. In order to test this hypothesis, we aimed to visualize the localization of the Innexin7 protein. As the antibody against *Drosophila* Innexin7 recognizes a peptide stretch that is not present in the *Tribolium* Inx7a (Supplementary Fig. S2), we designed a Tc-Inx7a-V5 fusion protein, injected its mRNA into early wild type eggs and performed immunohistochemistry using an antibody against the V5 tag. The transiently expressed protein was detected in 15 out of 45 injected eggs and is indeed localized at the base of the invaginated membrane (Figure 11 A). This localization is observed when the tip of the invaginated membrane started to enlarge and split between the cells (Figure 11 A). This stage coincides with the delaminating protocells following Tc-inx7a pRNAi. Finally, during actual basal cell closure, Inx7a-V5 localizes all over the forming basal membrane in plaques typical for gap junctions (Figure 11 B, C) (52). This stage coincides with the retraction of the membranes following Tc-inx7a RNAi. We propose that Innexin7a forms gap junctions between the nascent basal cell membrane and the yolk plasmalemma, stabilizing the forming basal membrane.

Discussion and conclusions

We have described cellularization in the beetle *Tribolium castaneum* and identified junctions joining together the laterally extending basal membrane and the forming yolk plasmalemma. In a functional screen for junction proteins, we found a critical role for Inx7 in cellularization. When Tc-inx7a is depleted maternally, the basal cell membranes do not form and the ingressed plasma membrane retracts to the apical surface at the time basal cell closure starts. We propose that Inx7a is a component of the newly identified junctions that stabilize the ingressed membrane.

Differences in Tribolium and Drosophila cellularization

Cellularization in *Tribolium* exhibits six remarkable differences to *Drosophila*. First, the plasma membrane does not retract during divisions as in *Drosophila*. Second, cell closure in *Tribolium* appears to take place one cell cycle earlier than in *Drosophila*, i.e. after the 12th instead of the 13th division (1, 2, 53, 54). This difference is not surprising, as variation in the number and rate of nuclear divisions is common among insect groups (55). Third, the furrow canals are not enriched with actin.

Fourth, in *Drosophila*, the phase of slow membrane extension is accompanied by elongation of the nuclei and is followed by a phase of rapid membrane extension allowing deep ingression before final closure of the cell (4). In *Tribolium*, the nuclei remain spherical, and the rapid phase is absent. After the last synchronous division, the membrane does not extend any further (Figure 12 A), and cell closure directly follows (Figure 12 B, C) leading to a much thinner blastoderm with cuboidal cells. Cells of the embryonic ectoderm then elongate and form a pseudostratified columnar epithelium (13, 56). This is similar to most insect lineages studied, including basally branching insects, and is therefore likely to be ancestral (55, 57). In contrast, a thickened layer of cytoplasm with apically positioned nuclei has evolved in *Drosophila* and other Cyclorrhapha (higher Diptera) (58). Thus, the membrane has to ingress much further, requiring a long phase of rapid extension. As a result, cellularization in *Drosophila* directly yields columnar cells. This may facilitate more rapid development, as it has been suggested

that cuboidal cells first have to elongate before gastrulation, whereas columnar cells can directly enter gastrulation (58).

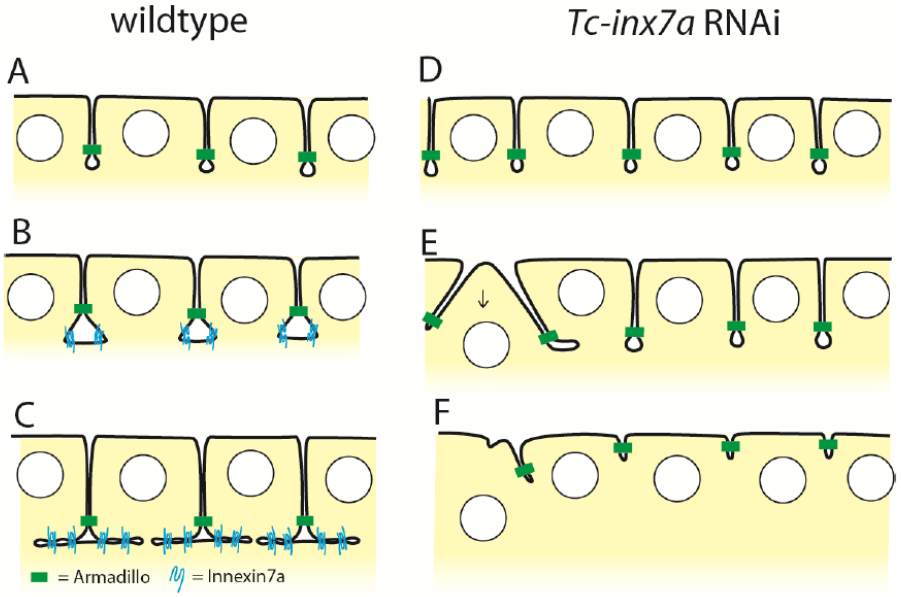

Figure 12. Model for a role of Inx7a in cellularization in Tribolium *(**A-C**) wild type cellularization. **(A)** Membrane invaginates between the nuclei after the 10th nuclear division and remains at this depth. Furrow canals and basal adherens junctions (green) form. **(B, C)** Inx7a forms junctions in the enlarging furrow canal mediating the splitting of the tip of the ingressed membrane (C). Inx7a forms gap junctions joining together the nascent basal cell membrane and the forming yolk plasmalemma stabilizing the ingressed membrane and enabling basal cell closure. (**D-F**) Tc-inx7a pRNAi severely affects cellularization. **(D)** Membrane invaginates normally in Tc-inx7a pRNAi embryos and basal adherens junctions form (green). **(E)** In absence of Inx7a, the tip of the ingressed membrane does not split properly. Ingressed membrane of a protocell can be inclined toward neighboring nuclei, this particular protocell will be extruded from the epithelium. **(F)** Finally, ingressed membrane retracts to the apical surface, as the membrane is not stabilized.*

Fifth, basal cell closure appears to take place through different mechanisms in *Drosophila* and *Tribolium*. Interestingly, in *Drosophila*, basal cell closure is mediated by contractile actin rings (1). We could not visualize such rings in *Tribolium* using either LifeAct-GFP live imaging or immunohistochemistry with an anti-actin antibody, whereas the latter method did reveal these rings in *Drosophila* (supplementary Fig. 1F). The microtubules visible in TEM micrographs and tubulin antibody stains, and the moving GAP43-positive vesicles, suggest the possibility that polarized membrane insertion may be a driving force involved in basal cell closure in *Tribolium*, similar to the fast phase of membrane extension in *Drosophila*.

However, the exact forces involved in basal cell closure in *Tribolium* remain to be elucidated.

Sixth, we found junctions that keep together the forming basal membrane and the forming yolk membrane. Such junctions have not been described in *Drosophila*. It seems that these junctions are instrumental in basal cell closure in *Tribolium*.

RNA deep sequencing

The method called parental RNAi (pRNAi) is used standardly in *Tribolium* and a few other insects to silence genes (59). It is systemic, highly penetrant and it can phenocopy genetic null phenotypes (31, 60). In contrast, in other organism other techniques are used to silence genes instead of pRNAi, such as canonical RNAi, mutagenesis or morpholino injections (61). These methods have been shown to trigger complex feedback mechanisms especially when paralogues genes are present. Recently, it has been shown that Non-sense Mediated Decay (NMD) caused by various mutations has a complex effect on the expression of many other genes in various organism (62). The mechanism of NMD is not yet understood, but it has not been reported yet for morpholino gene knockdown approaches. Hashimoto, et al found that there is a machinery to clear mRNA 5'-fragments produced by both RNAi and NMD in *D. melanogaster* cells (63). In yeast it was shown that this machinery, called nonstop mRNA decay (NSD), triggers nonstop mRNA degradation by removing stalled ribosomes (62). In *Tribolium* NMD after gene silencing using pRNAi has not been studied yet. Rehwinkel et al (63) studied the role of the argonaut proteins during NMD in *D. melanogaster*, but concluded that the mechanism is still not well understood. When a gene is knocked down using pRNAi, the mRNA is degraded by the RISC complex (65). It is possible that NMD works via the RISC complex, or the RISC complex might leave bits of RNA which triggers NMD. To further investigate complex feedback processes, including the effects of NSD, at the transcriptome level after pRNAi we performed RNAseq experiments after knockdown of inx7a. Especially since inx7a has two highly similar paralogs, complex feedback mechanisms could be expected.

The effects of pRNAi knockdown of inx7a on the transcriptome of eggs is very strong on a large set of genes (Figure 10). In line with the strong

developmental effects of the knock down. Unexpectedly, the results show that inx7a is upregulated after knock down, this means that there is no evidence of the penetrance of the silencing or NMD based on the RNA level of the targeted gene itself (Table 3). We also see a strong up regulation effect of the pRNAi of inx7a on several other innexin genes. We found that 5 out of the 8 studied innexins where upregulated by silencing inx7 (innexins 1, 2, 456 and splice form 2 of innexin 8). The only gene of which the RNA level is significantly down regulated is inx3. The down regulation of innexin 7b, although not statistically significant, could be explained by a direct effect of the silencing since it has a similar sequence to innexin inx7a. The results show a complex feedback mechanism. It would be interesting to further investigate whether this is the result of NMD mechanisms or indirect feedback loops at the gene transcription regulation machinery level.

By performing gene enrichment analysis using DAVID or PathVisio software, we found many enriched pathways with a P-value adjusted value of p-value < 0.05. We show six pathways with the most significant values in the shown parameters. Considering that the RNAi targeting of inx7a resulted in severe developmental differences, it is very likely that many effects at the RNA level are indirectly caused by in difference in developmental timing. Comparing the two lists resulting from using the two software programs, the enriched pathways are different and their parameters have different values. We took the two pathways, DNA replication and notch that are present in both the DAVID and PathVisio list with significant parameter values for more detailed analysis (Figure 8 and Figure 9). Interestingly, a paper by Lechner, et al (66) showed a connection between inx2, wingless, Delta/Notch and hedgehog signaling. They found that hedgehog signaling is essential for the expression of wingless and Delta/Notch. Hedgehog and wingless regulate gap junction communication by transcriptionally activating the inx2 gene. In a feedback loop, inx2 is needed for the transcriptional activation of hedgehog, wingless and Delta/Notch (66). In summary, we used RNAseq to perform enrichment analysis of pathways after innexin 7a pRNAi targeting showing a very strong effect in many pathways. There are no published connections of innexins with signaling pathways described in any species. Therefore, our results could be the basis for future endeavors resulting in such a pathway.

The function of Innexin 7

The phenotype upon Tc-inx7a knock down demonstrates a role for the Inx7 group in stabilization of the ingressed plasma membrane after the 12th nuclear division. Furthermore, the localization of Inx7a-V5 suggests that Inx7a forms newly identified junctions between the forming basal membrane and the yolk membrane. We propose that these Inx7a-based junctions convey stability to the ingressed plasma membrane in two ways. First, these junctions split the leading edges (furrow canals) of the ingressed membrane immediately after the 12th division (Figure 12 B). In the absence of proper splitting, membrane of a protocell can become skewed towards neighboring nuclei, as happens during protocell delamination (Figure 12 E). Second, these junctions stabilize the forming basal membrane during the phase of actual basal cell closure (Figure 12C). Absence of this stabilization leads to the retraction of the ingresses membrane to the apical surface (Figure 12 F), causing a complete reversal of the cellularization process.

As Inx7 proteins are gap junction proteins, we suggest that the newly identified junctions are gap junctions, and that Inx7a is a key component of them. However, this remains to be proven, as Innexins can also function in a hemichannel (67). It is also possible that the newly identified junctions are of completely different nature, and that Inx7a is merely involved in their initial assembly or stabilization. Our RNAseq results showing the effect of our pRNAi approach indicate a possible connection of inx7 with DNA replication. In this context, the publication of Doble et al (2004) that shows that phosphorylation of serine 262 in the gap junction protein connexin-43 regulates DNA synthesis in human cardiomyocytes supports our findings. It is therefore interesting to further investigate the role of gap junction regulation in the DNA replication process.

It might seem surprising that the sole depletion of Inx7a shows this strong cellularization phenotype, while Tc-inx1, inx2, inx3, inx456 are also expressed during cellularization. However, specific protein properties might distinguish the Innexin7 paralogs from the other expressed Innexins. For instance, Inx7a, b and c display a distinctive Trp196 at the beginning of TM3 (Supplementary Fig. S2), a position involved in the oligomerization compatibility of the vertebrate Connexin43 (68). This Trp residue is also conserved in *Nasonia, Apis* and *Anopheles* Inx7. It is also possible that the Inx7a primes and stabilizes formation of heteromeric gap junctions with

other Innexins. This has been proposed for *Drosophila* Inx3 in a Inx1/2/3 complex in the amnioserosa, as the sole loss of Inx3 leads to a strong dorsal closure phenotype, in contrast to individual loss of Inx1 or Inx2 (69). Since in other organisms, paralogs often develop to have a specialized function in heteromeric complexes (e.g. reference Toll-like receptors heterodimers) it wouldn't be surprising if the paralogs of the innexin 7 group are forming heteromeric gap junctions and therefore have an equally important function.

The proposed mechanism of basal cell closure involving Inx7 could be unique to *Tribolium*. However, since the *Drosophila* mode of cellularization involving columnar cells is evolutionary derived, it seems more likely that the Inx7-mediated process is ancestral.

Contribution

Tania Vazquez-Faci: Writing, pRNAi experiments, sample collection and quality control, for transcriptional analysis, RNAseq and subsequent bioinformatic analysis.
Mathew A. Benton: time laps movies, injection of the inx7a-V5 fusion construct and subsequent egg fixation, writing of the manuscript.
Gerda E.M. Lamers: Transmission electron images.
Catherine Rabouille: writing and experimental analysis, initial concepts.
Herman Spaink: writing, RNAseq and subsequent bioinformatic analysis
Maurijn van der Zee: writing, immuno-histochemistry, egg fixation, phylogenetic analysis, pRNAi (RNAi screen and innexin experiments) experimental analysis, final supervision, initial concepts.

References

1. Harris, T.J.C., J.K. Sawyer, and M. Peifer. 2009. How the cytoskeleton helps build the embryonic body plan: Models of morphogenesis from Drosophila. Curr. Top. Dev. Biol. 89: 55–85.
2. Lecuit, T. 2004. Junctions and vesicular trafficking during Drosophila cellularization. J. Cell Sci. 117: 3427–3433.
3. Mazumdar, A., and M. Mazumdar. 2002. How one becomes many: blastoderm cellularization in Drosophila melanogaster. Bioessays. 24: 1012–22.
4. Schejter, E.D., and E. Wieschaus. 1993. Functional elements of the cytoskeleton in the early Drosophila embryo. Annu. Rev. Cell Biol. 9: 67–99.
5. Warn, R.M., and R. Magrath. 1983. Experimental Cell Research 143 (1983) 103-114 Distribution during the cellulari2ation with fl-phalloidin of the drosophila embryo visualized Exp. Cell Res. 143.
6. Lecuit, T., and E. Wieschaus. 2000. Polarized insertion of new membrane from a cytoplasmic reservoir during cleavage of the Drosophila embryo. J. Cell Biol.150 (4): 849-860.
7. Pelissier, A., J.P. Chauvin, and T. Lecuit. 2003. Trafficking through Rab11 Endosomes Is Required for Cellularization during Drosophila Embryogenesis. Curr. Biol. 13 (21): 1848-1857.
8. Riggs, B., W. Rothwell, S. Mische, G.R.X. Hickson, J. Matheson, T.S. Hays, G.W. Gould, and W. Sullivan. 2003. Actin cytoskeleton remodeling during early Drosophila furrow formation requires recycling endosomal components Nuclear-fallout and Rab11. J. Cell Biol. 163: 143–154.
9. Rothwell, W.F., P. Fogarty, C.M. Field, and W. Sullivan. 1998. Nuclear-fallout, a Drosophila protein that cycles from the cytoplasm to the centrosomes, regulates cortical microfilament organization. Development. 125(7):1295-303.
10. Sokac, A.M., and E. Wieschaus. 2008. Local Actin-Dependent Endocytosis Is Zygotically Controlled to Initiate Drosophila Cellularization. Dev. Cell. 14(5):775-786.
11. Schröder, R., A. Beermann, N. Wittkopp, and R. Lutz. 2008. From development to biodiversity - Tribolium castaneum, an insect model organism for short germband development. Dev. Genes Evol. 218:

119–126.
12. Handel, K., C.G. Grünfelder, S. Roth, and K. Sander. 2000. Tribolium embryogenesis: a SEM study of cell shapes and movements from blastoderm to serosal closure. Dev. Genes Evol. 210: 167–179.
13. Benton, M. a, M. Akam, and A. Pavlopoulos. 2013. Cell and tissue dynamics during Tribolium embryogenesis revealed by versatile fluorescence labeling approaches. Development. 140: 3210–20.
14. Bauer, R., B. Löer, K. Ostrowski, J. Martini, A. Weimbs, H. Lechner, and M. Hoch. 2005. Intercellular communication: The Drosophila innexin multiprotein family of gap junction proteins. Chem. Biol. 12: 515–526.
15. Ostrowski, K., R. Bauer, and M. Hoch. 2008. The Drosophila Innexin7 gap junction protein is required for development of the embryonic nervous system. Cell Commun. Adhes. 15: 155–167.
16. Phelan, P. 2005. Innexins: Members of an evolutionarily conserved family of gap-junction proteins. Biochim. Biophys. Acta - Biomembr. 1711: 225–245.
17. Abascal, F., and R. Zardoya. 2013. Evolutionary analyses of gap junction protein families. Biochim. Biophys. Acta - Biomembr.
18. Baranova, A., D. Ivanov, N. Petrash, A. Pestova, M. Skoblov, I. Kelmanson, D. Shagin, S. Nazarenko, E. Geraymovych, O. Litvin, A. Tiunova, T.L. Born, N. Usman, D. Staroverov, S. Lukyanov, and Y. Panchin. 2004. The mammalian pannexin family is homologous to the invertebrate innexin gap junction proteins. Genomics.
19. Wakimoto, B.T., F.R. Turner, and T.C. Kaufman. 1984. Defects in embryogenesis in mutants associated with the antennapedia gene complex of Drosophila melanogaster. Dev. Biol.
20. Panchina, Y., I. Kelmanson, M. Matz, K. Lukyanov, N. Usman, and S. Lukyanov. 2000. A ubiquitous family of putative gap junction molecules [2]. Curr. Biol. 10(13): 473-474.
21. Alexopoulos, H., A. Böttger, S. Fischer, A. Levin, A. Wolf, T. Fujisawa, S. Hayakawa, T. Gojobori, J.A. Davies, C.N. David, and J.P. Bacon. 2004. Evolution of gap junctions: The missing link? [1]. Curr. Biol. .
22. D'hondt, C., R. Ponsaerts, H. De Smedt, G. Bultynck, and B. Himpens. 2009. Pannexins, distant relatives of the connexin family with specific cellular functions? BioEssays.
23. Goodenough, D.A., and D.L. Paul. 2009. Gap junctions. Cold Spring

Harb. Perspect. Biol.
24. Meşe, G., G. Richard, and T.W. White. 2007. Gap junctions: Basic structure and function. J. Invest. Dermatol.
25. Scemes, E., S.O. Suadicani, G. Dahl, and D.C. Spray. 2007. Connexin and pannexin mediated cell-cell communication. In: Neuron Glia Biology.
26. Phelan, P., and T.A. Starich. 2001. Innexins get into the gap. BioEssays. 23: 388–396.
27. Güiza, J., I. Barría, J.C. Sáez, and J.L. Vega. 2018. Innexins: Expression, regulation, and functions. Front. Physiol. 9: 1–9.
28. Hughes, A.L. 2014. Evolutionary Diversification of Insect Innexins. J. Insect Sci. 14: 1–5.
29. Wu, C.L., M.F.M. Shih, J.S.Y. Lai, H.T. Yang, G.C. Turner, L. Chen, and A.S. Chiang. 2011. Heterotypic gap junctions between two neurons in the drosophila brain are critical for memory. Curr. Biol. 21: 848–854.
30. Panfilio, K.A., G. Oberhofer, and S. Roth. 2013. High plasticity in epithelial morphogenesis during insect dorsal closure. Biol. Open. 2: 1108–1118.
31. Bucher, G., J. Scholten, and M. Klingler. 2002. Parental RNAi in tribolium (coleoptera). Curr. Biol. 12: 85–86.
32. Altschul, S.F., T.L. Madden, A.A. Schäffer, J. Zhang, Z. Zhang, W. Miller, and D.J. Lipman. 1997. Gapped BLAST and PSI-BLAST: A new generation of protein database search programs. Nucleic Acids Res. 25(17): 3389–3402.
33. Galtier, N., M. Gouy, and C. Gautier. 1996. Seaview and phylo_ win: Two graphic tools for sequence alignment and molecular phylogeny. Bioinformatics. 12: 543–548.
34. Abascal, F., R. Zardoya, and D. Posada. 2005. ProtTest: Selection of best-fit models of protein evolution. Bioinformatics. .
35. Guindon, S., and O. Gascuel. 2003. A Simple, Fast, and Accurate Algorithm to Estimate Large Phylogenies by Maximum Likelihood. Syst. Biol. 52: 696–704.
36. Kumar, S., K. Tamura, and M. Nei. 2004. MEGA3: Integrated software for Molecular Evolutionary Genetics Analysis and sequence alignment. Brief. Bioinform. 5: 150–163.
37. Van Der Zee, M., N. Berns, and S. Roth. 2005. Distinct functions of

the Tribolium zerkn??llt genes in serosa specification and dorsal closure. Curr. Biol. 15: 624–636.
38. Zee, M. v. d., O. Stockhammer, R.N. d. Fonseca, C. v. Levetzow, and S. Roth. 2006. Sog/Chordin is required for ventral-to-dorsal Dpp/BMP transport and head formation in a short germ insect. Proc. Natl. Acad. Sci. 103: 16307–16312.
39. Veneman, W.J., J. de Sonneville, K.J. van der Kolk, A. Ordas, Z. Al-Ars, A.H. Meijer, and H.P. Spaink. 2015. Analysis of RNAseq datasets from a comparative infectious disease zebrafish model using GeneTiles bioinformatics. Immunogenetics. 67: 135–147.
40. Da Wei Huang, Brad T Sherman, L.R. 2009. Systematic and integrative analysis of large gene lists using DAVID bioinformatics resources. Nat. Protoc. 4: 44–57.
41. Huang DW, Sherman BT, L.R. 2009. Bioinformatics enrichment tools: paths toward the comprehensive functional analysis of large gene lists. Nucleic Acids Res. 37: 1–13.
42. Martina Kutmon, Martijn P. van Iersel, Anwesha Bohler, Thomas Kelder, Nuno Nunes, Alexander R. Pico, C.T.E. 2015. PathVisio 3: An Extendable Pathway Analysis Toolbox. PLoS Comput ational Biol. 11.
43. Mavrakis, M., O. Pourquié, and T. Lecuit. 2010. Lighting up developmental mechanisms: how fluorescence imaging heralded a new era. Development. 137: 373–387.
44. Sarrazin, A.F., A.D.Peel, and M. Averof. 2012. A Segmentation Clock with Two-Segment periodicity in insects. Science (80-.). : 338–342.
45. van Drongelen, R., T. Vazquez-Faci, T.A.P.M. Huijben, M. van der Zee, and T. Idema. 2018. Mechanics of epithelial tissue formation. J. Theor. Biol. 454: 182–189.
46. Riedl, J., A.H. Crevenna, K. Kessenbrock, J.H. Yu, D. Neukirchen, M. Bista, F. Bradke, D. Jenne, T.A. Holak, Z. Werb, M. Sixt, and R. Wedlich-Soldner. 2008. Lifeact: a versatile marker to visualize F-actin. Nat. Methods. 5: 605–607.
47. van der Zee, M., M.A. Benton, T. Vazquez-Faci, G.E.M. Lamers, C.G.C. Jacobs, and C. Rabouille. 2015. Innexin7a forms junctions that stabilize the basal membrane during cellularization of the blastoderm in Tribolium castaneum. Development. 142: 2173–2183.
48. Recolin, B., S. van der Laan, N. Tsanov, and D. Maiorano. 2014.

Molecular mechanisms of DNA replication checkpoint activation. Genes (Basel). 5: 147–175.
49. Kopan, R., and M.X.G. Ilagan. 2009. The Canonical Notch Signaling Pathway: Unfolding the Activation Mechanism. Cell. 137: 216–233.
50. Bauer, R., C. Lehmann, J. Martini, F. Eckardt, and M. Hoch. 2004. Gap junction channel protein Innexin 2 is essential for epithelial morphogenesis in the Drosophila embryo. Mol. Biol. Cell. 15(6):2992-3004.
51. Zhang, C.X., M.P. Lee, A.D. Chen, S.D. Brown, and T.S. Hsieh. 1996. Isolation and characterization of a Drosophila gene essential for early embryonic development and formation of cortical cleavage furrows. J. Cell Biol. 134(4):923-34.
52. Shestopalov, V.I., and Y. Panchin. 2008. Pannexins and gap junction protein diversity. Cell. Mol. Life Sci. 65(3):376-94.
53. Handel, K., C.G. Grünfelder, S. Roth, and K. Sander. 2000. Tribolium Embryogenesis 2000. : 167–179.
54. Mazumdar, A., and M. Mazumdar. 2002. How one becomes many: blastoderm cellularization in Drosophila melanogaster. BioEssays. 24: 1012–1022.
55. Anderson, D.T. 1972. The development of holometabolous insects. In Developmental Systems: Insects. London: Academic Press.
56. Handel, K., A. Basal, X. Fan, and S. Roth. 2005. Tribolium castaneum twist: Gastrulation and mesoderm formation in a short-germ beetle. Dev. Genes Evol. 215: 13–31.
57. EDE, D.A. 1964. an Inherited Abnormality Affecting the Development of the Yolk. J. Embryol. Exp. Morphol. 12: 551–562.
58. Bullock, S.L., M. Stauber, A. Prell, J.R. Hughes, D. Ish-Horowicz, and U. Schmidt-Ott. 2004. Differential cytoplasmic mRNA localisation adjusts pair-rule transcription factor activity to cytoarchitecture in dipteran evolution. Development. 131: 4251–4261.
59. Berghammer, A.J., M. Weber, J. Trauner, and M. Klingler. 2009. Red flour beetle (Tribolium) germline transformation and insertional mutagenesis. Cold Spring Harb. Protoc. 4: 1–18.
60. Posnien, N., J. Schinko, D. Grossmann, T.D. Shippy, B. Konopova, and G. Bucher. 2009. RNAi in the red flour beetle (Tribolium). Cold Spring Harb. Protoc. 4.
61. Horn, C., and E. a. Wimmer. 2000. A versatile vector set for animal

transgenesis. Dev. Genes Evol. 210: 630–637.
62. S. Javad Rasouli & Didier Y.R. Stainier. 2017. Regulation of cardiomyocyte behavior in zebrafish trabeculation by Neuregulin 2a signaling. Nat. Commun. 8.
63. Hashimoto, Y., M. Takahashi, E. Sakota, and Y. Nakamura. 2017. Nonstop-mRNA decay machinery is involved in the clearance of mRNA 5'-fragments produced by RNAi and NMD in Drosophila melanogaster cells. Biochem. Biophys. Res. Commun. 484(1):1-7.
64. Rehwinkel, J., I. Behm-Ansmant, D. Gatfield, and E. Izaurralde. 2005. A crucial role for GW182 and the DCP1:DCP2 decapping complex in miRNA-mediated gene silencing. Rna. 11: 1640–1647.
65. White, B. 2007. Recombinant DNA: Genes and genomes—A short course (3rd ed.). Biochem. Mol. Biol. Educ.
66. Lechner, H., F. Josten, B. Fuss, R. Bauer, and M. Hoch. 2007. Cross regulation of intercellular gap junction communication and paracrine signaling pathways during organogenesis in Drosophila. Dev. Biol. 310: 23–34.
67. Scemes, E., D.C. Spray, and P. Meda. 2009. Connexins, pannexins, innexins: Novel roles of "hemi-channels." Pflugers Arch. Eur. J. Physiol. 457(6):1207-1226.
68. Largrée, V., K. Brunschwig, P. Lopez, N.B. Gilula, G. Richard, and M.M. Falk. 2003. Specific amino-acid residues in the N-terminus and TM3 implicated in channel function and oligomerization compatibility of connexin43. J. Cell Sci. 116: 3189–3201.
69. Giuliani, F., G. Giuliani, R. Bauer, and C. Rabouille. 2013. Innexin 3, a New Gene Required for Dorsal Closure in Drosophila Embryo. PLoS One. 8: 1–16.
70. Käll, L., A. Krogh, and E.L.L. Sonnhammer. 2005. An HMM posterior decoder for sequence feature prediction that includes homology information. Bioinformatics. 1:251-257 .
71. Richards, S., R. a Gibbs, G.M. Weinstock, S.J. Brown, R. Denell, R.W. Beeman, R. Gibbs, R.W. Beeman, S.J. Brown, G. Bucher, M. Friedrich, C.J.P. Grimmelikhuijzen, M. Klingler, M. Lorenzen, S. Richards, S. Roth, R. Schröder, D. Tautz, E.M. Zdobnov, D. Muzny, R. a Gibbs, G.M. Weinstock, T. Attaway, S. Bell, C.J. Buhay, M.N. Chandrabose, D. Chavez, K.P. Clerk-Blankenburg, A. Cree, M. Dao, C. Davis, J. Chacko, H. Dinh, S. Dugan-Rocha, G. Fowler, T.T. Garner, J. Garnes,

A. Gnirke, A. Hawes, J. Hernandez, S. Hines, M. Holder, J. Hume, S.N. Jhangiani, V. Joshi, Z.M. Khan, L. Jackson, C. Kovar, A. Kowis, S. Lee, L.R. Lewis, J. Margolis, M. Morgan, L. V Nazareth, N. Nguyen, G. Okwuonu, D. Parker, S. Richards, S.-J. Ruiz, J. Santibanez, J. Savard, S.E. Scherer, B. Schneider, E. Sodergren, D. Tautz, S. Vattahil, D. Villasana, C.S. White, R. Wright, Y. Park, R.W. Beeman, J. Lord, B. Oppert, M. Lorenzen, S. Brown, L. Wang, J. Savard, D. Tautz, S. Richards, G. Weinstock, R. a Gibbs, Y. Liu, K. Worley, G. Weinstock, C.G. Elsik, J.T. Reese, E. Elhaik, G. Landan, D. Graur, P. Arensburger, P. Atkinson, R.W. Beeman, J. Beidler, S.J. Brown, J.P. Demuth, D.W. Drury, Y.-Z. Du, H. Fujiwara, et al. 2008. The genome of the model beetle and pest Tribolium castaneum. Nature. 452: 949–955.

72. Bucher, G., J. Scholten, and M. Klingler. 2002. Parental RNAi in Tribolium (Coleoptera). Curr. Biol. 12: R85–R86.

Supplementary data

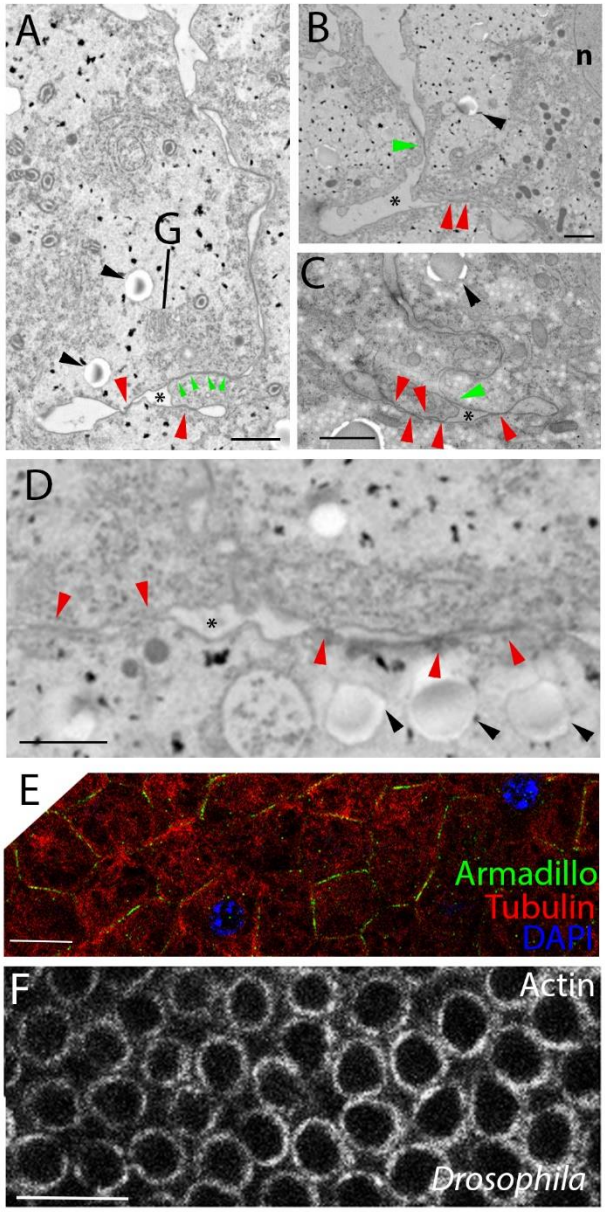

Figure S1. Novel junctions form along the basal membrane that are not adherens junctions (A-D) TEM visualization of both the lateral BAJ (green arrowheads) as well as novel junctions between the nascent basal cell membrane and the forming yolk plasmalemma (red arrowheads). Note that the number of junctions increases as the basal m embrane extends, until junctions are present along the whole basal membrane (D). Asterisks indicate the split furrow. Black arrowheads point at vesicles that could be lipid droplets. G denotes Golgi in (A). n denotes nucleus in (B) (E) Immunofluorescence (IF) visualization of Armadillo (green), Tubulin (red) and DAPI (blue) at the basal membrane towards the end of basal cell closure. Note that Armadillo is mainly detected between neighboring cells, not at the whole basal membrane. (F) IF visualization of actin at the bases of the cells in Drosophila.Note the conspicuous actin rings. Scale bars in (A-D): 1 µm. Scale bar in (E): and (F) 10 µm.

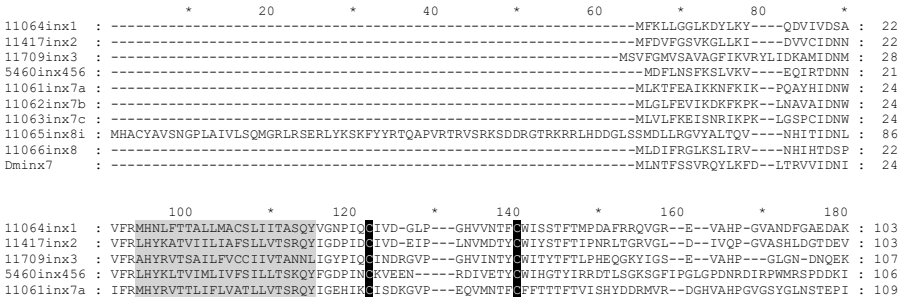

Figure S2 Alignment of the Tribolium Innexins with Drosophila Innexin 7 using Praline (http://www.ibi.vu.nl/programs/pralinewww). The four Transmembrane (TM) domains were predicted by Phobius (1) and are shaded in grey. The conserved YYQW motif in the first TM domain is indicated in white letters. The conserved C-residues in the extracellular loops are shaded in black. The peptide against which the Drosophila Innexin7 antibody was raised is underlined (2). A distinctive Trp residue at the beginning of TM3 is indicated in bold. 11065inx8i is an isoform of inx8 with alternative first exons.

Table S1 Results of the parental RNAi screen for cell adhesion genes

TCnumber	CGnumber	*Drosophila* name	general name	junction	phenotype of offspring after pupal injection	after adult injection
TC013706	CG1560	*myospheroid*	integrin-beta	focal	normal, 10% abnormal growth zones, 5% empty eggs	
TC013570	CG3722	*shotgun*	DE cadherin	adherens	mothers died	mothers died
TC014460	CG10624	*sinuous*	PMP-22/claudin	septate	sterile	sterile
TC014461	CG14779	*pickel*	PMP-22/claudin	septate	normal, 8% very inconsistent phenotypes	
TC014139	CG9326	*varicose*	PALS2	septate	sterile	sterile
TC014459	CG1298	*kune-kune*	PMP-22/claudin	septate	sterile	10% curved larvae
TC004424	CG6383	*crumbs*	crumbs	tight/apical	variety of strong phenotypes, strongly affected germband extension	
TC011064	CG3039	*ogre*	innexin1	gap	normal, 5% mild dorsal closure problems	
TC011417	CG4590	*kropf*	innexin2	gap	20% mild dorsal closure phenotypes, some curved larvae	
TC011709	CG1448	*inx3*	innexin3	gap	most eggs hatched, 6% strong impairment of morphogenetic movements	
TC005460	CG10125	*zero population growth*	innexin456	gap	10% mild dorsal closure phenotypes, some curved larvae	
TC011061	CG2977	*inx7*	innexin7a	gap	100% strong cellularization phenotype	
TC011062			innexin7b	gap	normal	
TC011063			innexin7c	gap	not cloned	
TC011065/6	CG34358	*shak-B*	innexin8	gap	normal	

Potential orthologs of *Drosophila* cell adhesion molecules were identified with BLAST (3) in the genome of *Tribolium castaneum (4).* A 500-600 bp fragment of these genes was cloned into pCRII-TOPO vector (Invitrogen) and sequenced for confirmation. PCR templates for dsRNA synthesis were generated with M13 primers, and dsRNA was synthesized using SP6 and T7 polymerases (Ambion). About 25 pupae were injected according to Bucher et al 2002 (5). If pupal RNAi was lethal or resulted in sterile adults, we injected adults directly according to van der zee 2006 (6), see last column. Eggs (usually around 60) were collected during a period of 3 days, fixed in a 4% formaldehyde/heptane mix and stained with DAPI. In addition to defects in cellularization, embryos were screened for general morphology and morphogenetic movements like gastrulation, germ band extension and dorsal closure. In addition, larvae or unhatched eggs were treated overnight with lactic acid and mounted for light microscopy. This screen is not exhaustive; for instance, another *myospheroid* (integrin-beta)

like gene (TC011707) is present in the *Tribolium* genome. Furthermore, actual knockdown (absence of the mRNA) was not verified, and phenotypes not visible by DAPI staining were obviously missed.

Table S3. ***Primers for inx7a RNAi fragments****. All primers are written 5'- 3'*

RNAi primer sets:		
inx7a fragment 1	CTGTCACGACTCTGGACGAA	CTCTTCGTCGCTCTCCAAAC
inx7a fragment 2	CGACGCTCCTAGTGACTTCC	ACCACCGAGACCAGGATTTA
inx7a fragment 3	CGACGCTCCTAGTGACTTCC	CTCTTCGTCGCTCTCCAAAC

Reference

1. Käll, L., A. Krogh, and E.L.L. Sonnhammer. 2005. An HMM posterior decoder for sequence feature prediction that includes homology information. Bioinformatics. 1:251-7.
2. Ostrowski, K., R. Bauer, and M. Hoch. 2008. The Drosophila Innexin7 gap junction protein is required for development of the embryonic nervous system. Cell Commun. Adhes. 15: 155–167.
3. Altschul, S.F., T.L. Madden, A.A. Schäffer, J. Zhang, Z. Zhang, W. Miller, and D.J. Lipman. 1997. Gapped BLAST and PSI-BLAST: A new generation of protein database search programs. Nucleic Acids Res. .
4. Richards, S., R. a Gibbs, G.M. Weinstock, S.J. Brown, R. Denell, R.W. Beeman, R. Gibbs, R.W. Beeman, S.J. Brown, G. Bucher, M. Friedrich, C.J.P. Grimmelikhuijzen, M. Klingler, M. Lorenzen, S. Richards, S. Roth, R. Schröder, D. Tautz, E.M. Zdobnov, D. Muzny, R. a Gibbs, G.M. Weinstock, T. Attaway, S. Bell, C.J. Buhay, M.N. Chandrabose, D. Chavez, K.P. Clerk-Blankenburg, A. Cree, M. Dao, C. Davis, J. Chacko, H. Dinh, S. Dugan-Rocha, G. Fowler, T.T. Garner, J. Garnes, A. Gnirke, A. Hawes, J. Hernandez, S. Hines, M. Holder, J. Hume, S.N. Jhangiani, V. Joshi, Z.M. Khan, L. Jackson, C. Kovar, A. Kowis, S. Lee, L.R. Lewis, J. Margolis, M. Morgan, L. V Nazareth, N. Nguyen, G. Okwuonu, D. Parker, S. Richards, S.-J. Ruiz, J. Santibanez, J. Savard,

S.E. Scherer, B. Schneider, E. Sodergren, D. Tautz, S. Vattahil, D. Villasana, C.S. White, R. Wright, Y. Park, R.W. Beeman, J. Lord, B. Oppert, M. Lorenzen, S. Brown, L. Wang, J. Savard, D. Tautz, S. Richards, G. Weinstock, R. a Gibbs, Y. Liu, K. Worley, G. Weinstock, C.G. Elsik, J.T. Reese, E. Elhaik, G. Landan, D. Graur, P. Arensburger, P. Atkinson, R.W. Beeman, J. Beidler, S.J. Brown, J.P. Demuth, D.W. Drury, Y.-Z. Du, H. Fujiwara, et al. 2008. The genome of the model beetle and pest Tribolium castaneum. Nature. 452: 949–955.

5. Bucher, G., J. Scholten, and M. Klingler. 2002. Parental RNAi in Tribolium (Coleoptera). Curr. Biol. 12: R85–R86.

6. Zee, M. v. d., O. Stockhammer, R.N. d. Fonseca, C. v. Levetzow, and S. Roth. 2006. Sog/Chordin is required for ventral-to-dorsal Dpp/BMP transport and head formation in a short germ insect. Proc. Natl. Acad. Sci. 103: 16307–16312.